Supplementary Information:

Supplementary figures, notes, and synthesis and characterization of compounds

This PDF file includes:

Supplementary Figures 1 through 15

Supplementary Notes 1 and 2

Compound Synthesis and Characterization

Table of Contents

Supplementary Fig. 1. Extended whole protein data for benchmarking experiments..... 3
Supplementary Fig. 2. Extended data for multiPSM workflow..... 4
Supplementary Fig. 3. Examples of spectra with varying levels of chimerism..... 5
Supplementary Fig. 4. Delta score ROC curves for probes 2-8..... 6
Supplementary Fig. 5. Number of PSMs per spectra ROC Curves for probes 2-8..... 6
Supplementary Fig. 6. Retention time ROC curves for probes 2-8..... 7
Supplementary Fig. 7. Final model ROC curves for probes 2-8..... 7
Supplementary Fig. 8. Additional examples of labeling events mapped to PDB structures..... 8
Supplementary Fig. 9. Extended proteomic data for TMT SoL pilot experiment..... 10
Supplementary Fig. 10. Correlation matrices from TMT dose SoL experiments..... 11
Supplementary Fig. 11. Supplementary proteomic data for TMT dose SoL experiments..... 13
Supplementary Fig. 12. Examples of proteome-wide, site-specific, concentration-dependent probe-protein interaction profiles 15
Supplementary Fig. 13. Examples of labeling events mapped to Alpha Fold structures 17
Supplementary Fig. 14. Docking analysis of diverse sites 19
Supplementary Fig. 15. Docking analysis of validated probe-protein interactions 21
Supplementary Note 1. Comparison of multiPSM search to ptmRS localization 23
Supplementary Note 2. Compound synthesis and characterization 23
References 29
NMR spectra 30

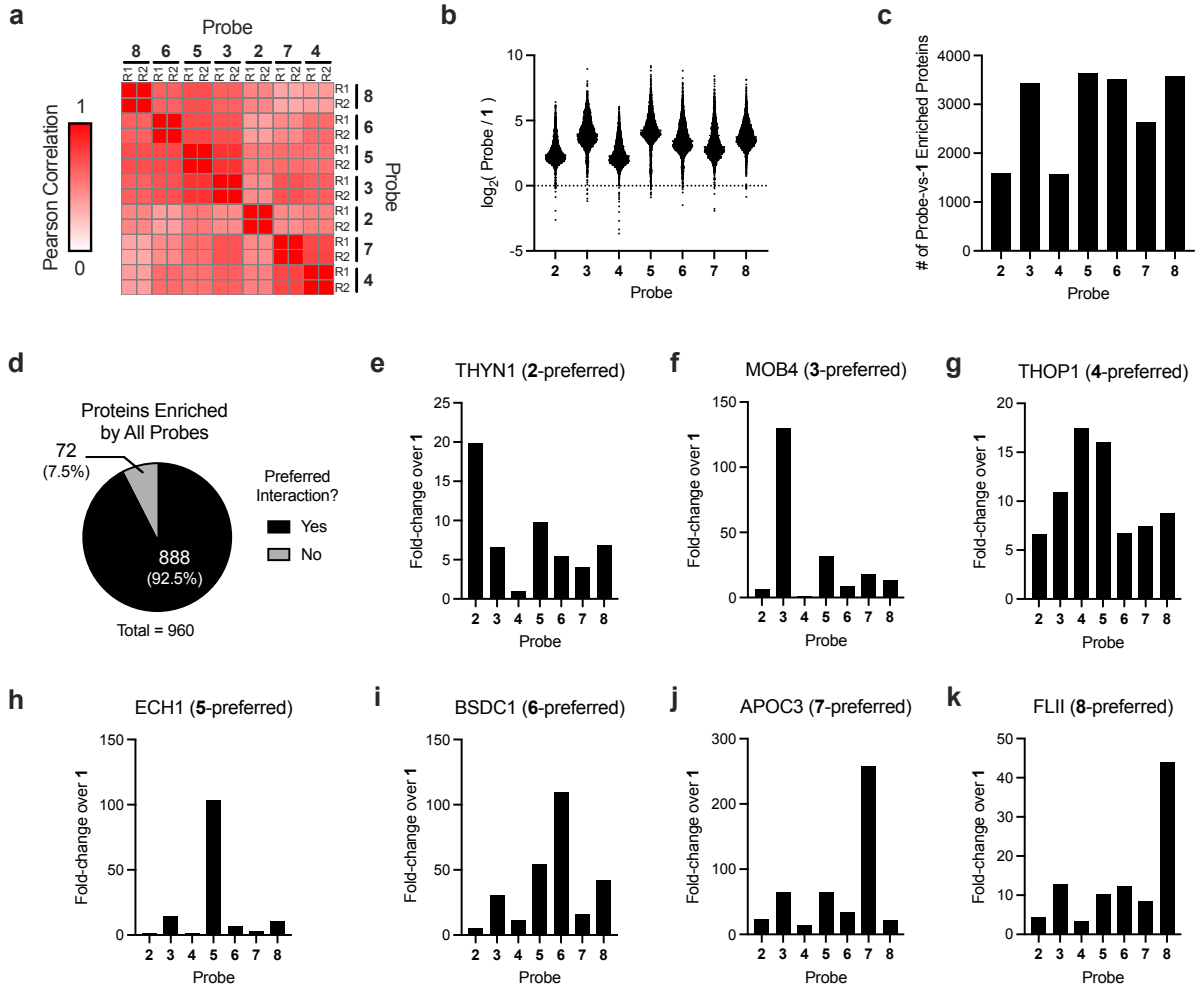

Supplementary Figure 1. Extended whole protein data for benchmarking experiments. (**a**) Correlation of protein quantitation from TMT experiments. (**b**) Fold-change of all quantified proteins over control probe **1** for each probe. (**c**) Number of proteins enriched by each probe over control probe **1** ($p < 0.05$, fold-change > 5). P-values for the abundance ratios were calculated using two-tailed Student's t-test with no adjustments for multiple comparisons. (**d**) Proportion of proteins enriched by all probes that show a preferred interaction with one or a subset of probes (>3-fold difference between minimum and maximum enrichment). (**e**-**k**) Examples of probe-preferred proteins for probes **2**-**8**.

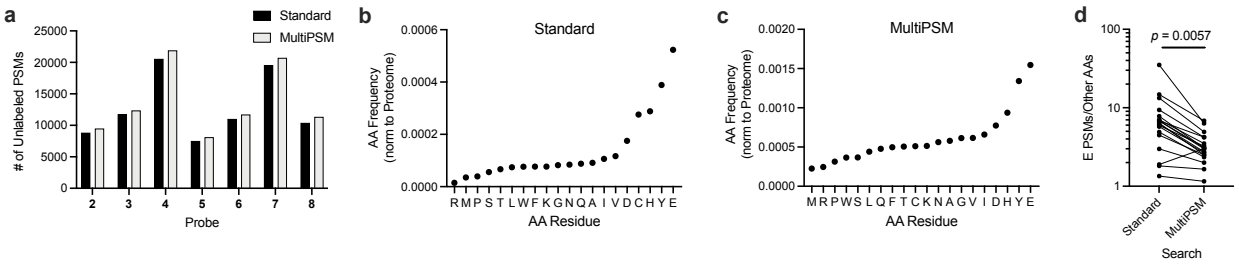

Supplementary Figure 2. Extended data for multiPSM workflow. (**a**) Unlabeled PSMs detected in standard and multiPSM proteomic searches. (**b**-**c**) Amino acid labeling frequency derived from standard (**b**) and multiPSM (**c**) searches (normalized to amino acid frequency in the *Homo sapiens* proteome used for the proteomic search). (**d**) Fold-change of PSMs assigning label location to “E” relative to all other amino acids (compared via two-sided paired t-test not corrected for multiple comparisons).

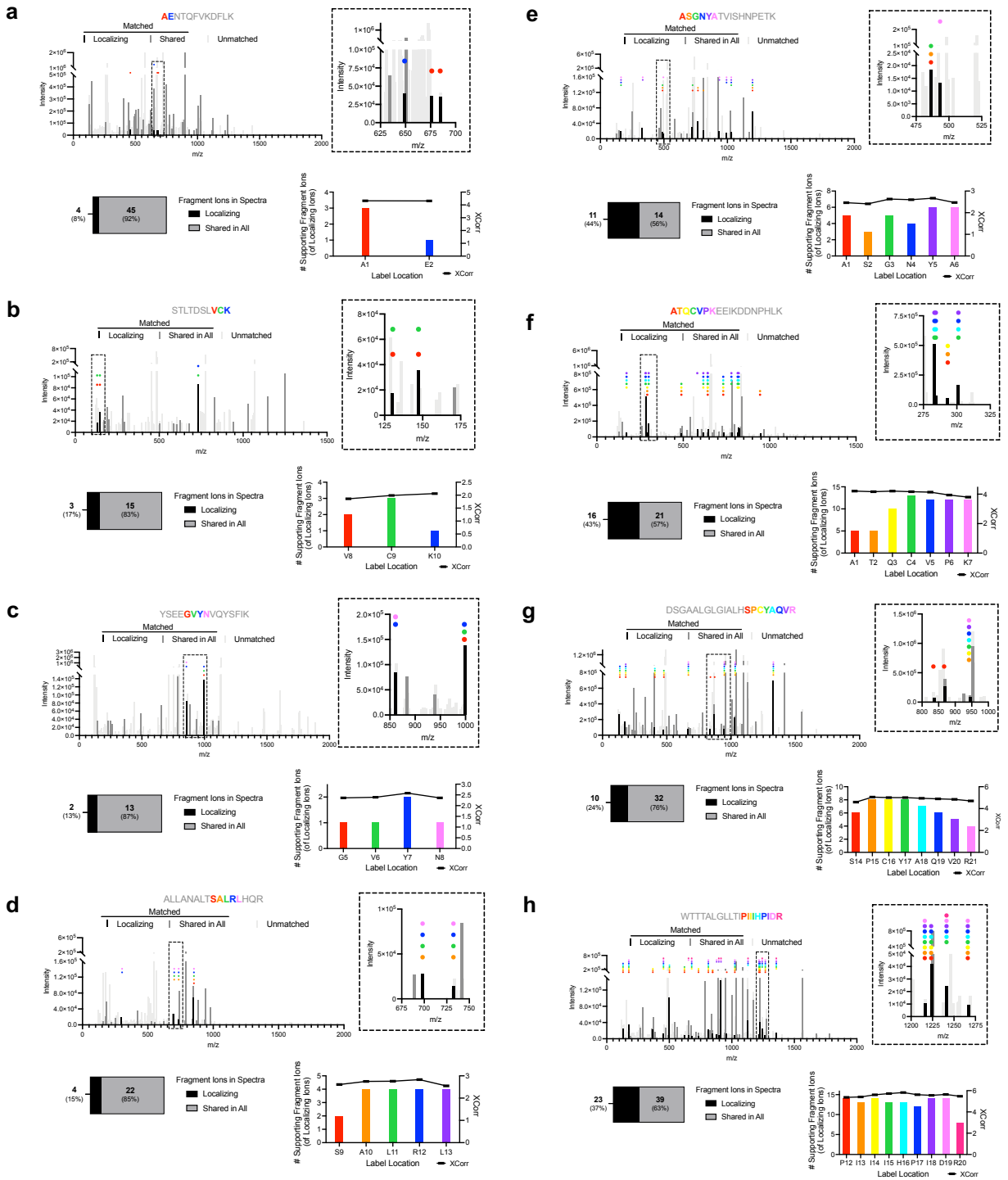

Supplementary Figure 3. Examples of spectra with varying levels of chimerism. Example of a chimeric spectra containing (**a**) two, (**b**) three, (**c**) four, (**d**) five, (**e**) six, (**f**) seven, (**g**) eight, and (**h**) nine label sites. For all plots, probe label sites and corresponding supporting fragment ions are indicated with identical colors. Insets show various zoomed regions of chimeric spectra. All plots include proportion of fragment ions in chimeric spectra that correspond to a particular probe location or are shared in all locations (lower left) and number of supporting fragment ions and XCorr values for each label location within the example chimeric spectra (lower right).

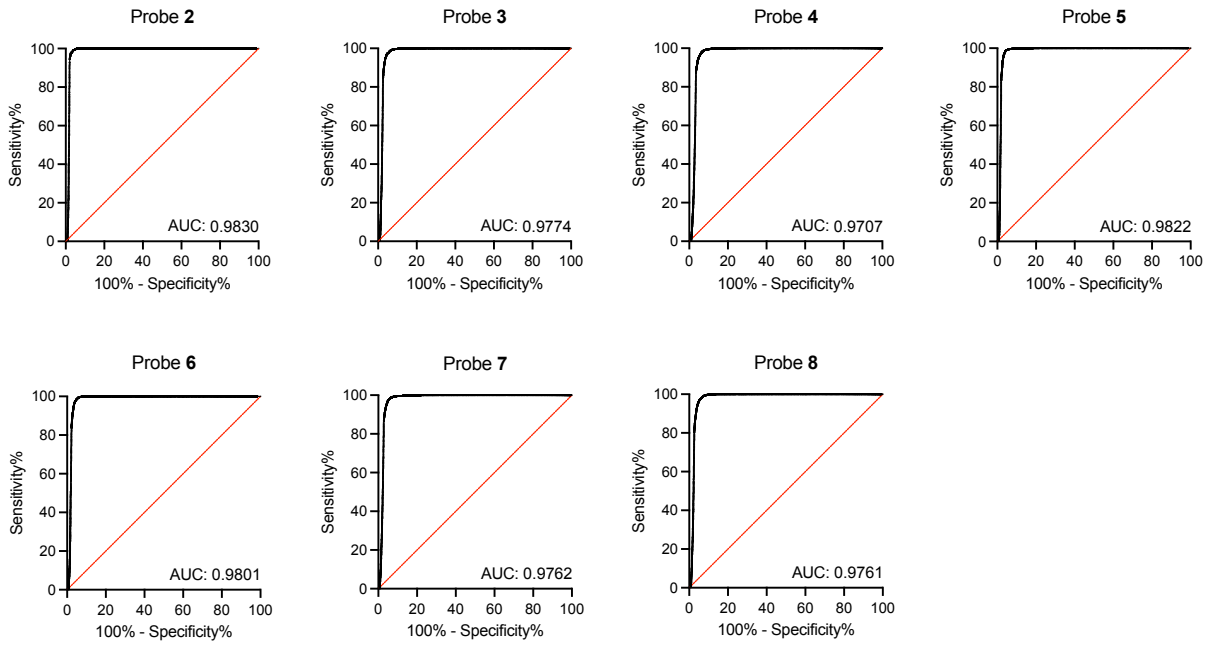

Supplementary Figure 4. Delta score ROC curves for probes **2**-**8**.

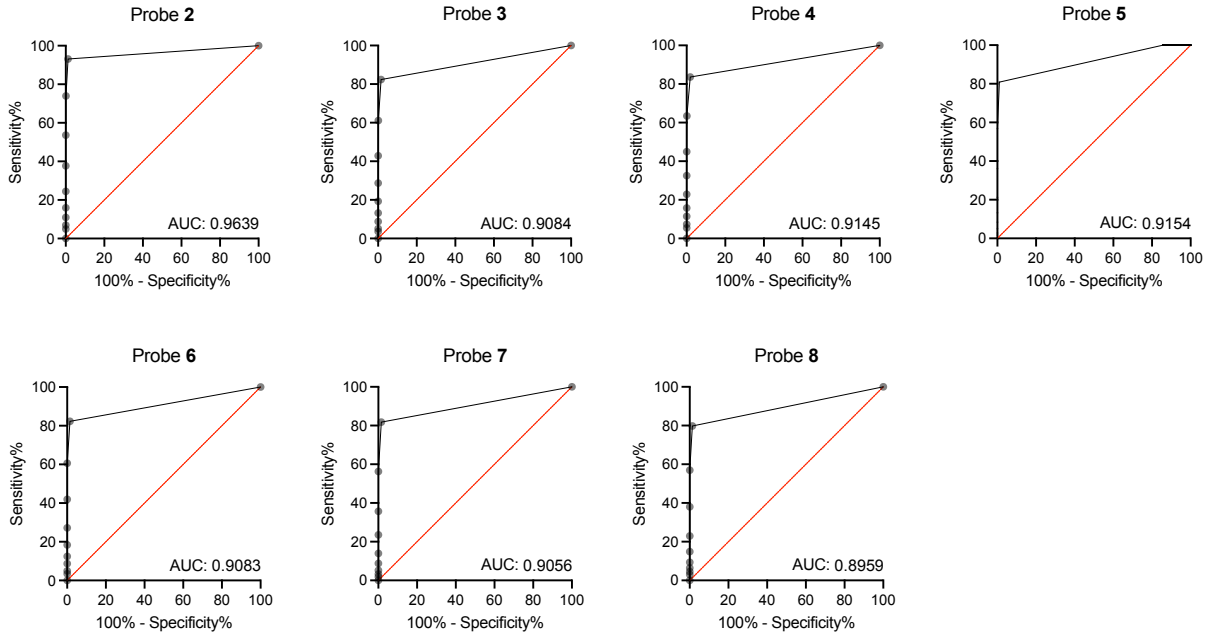

Supplementary Figure 5. Number of PSMs per spectra ROC Curves for probes **2**-**8**.

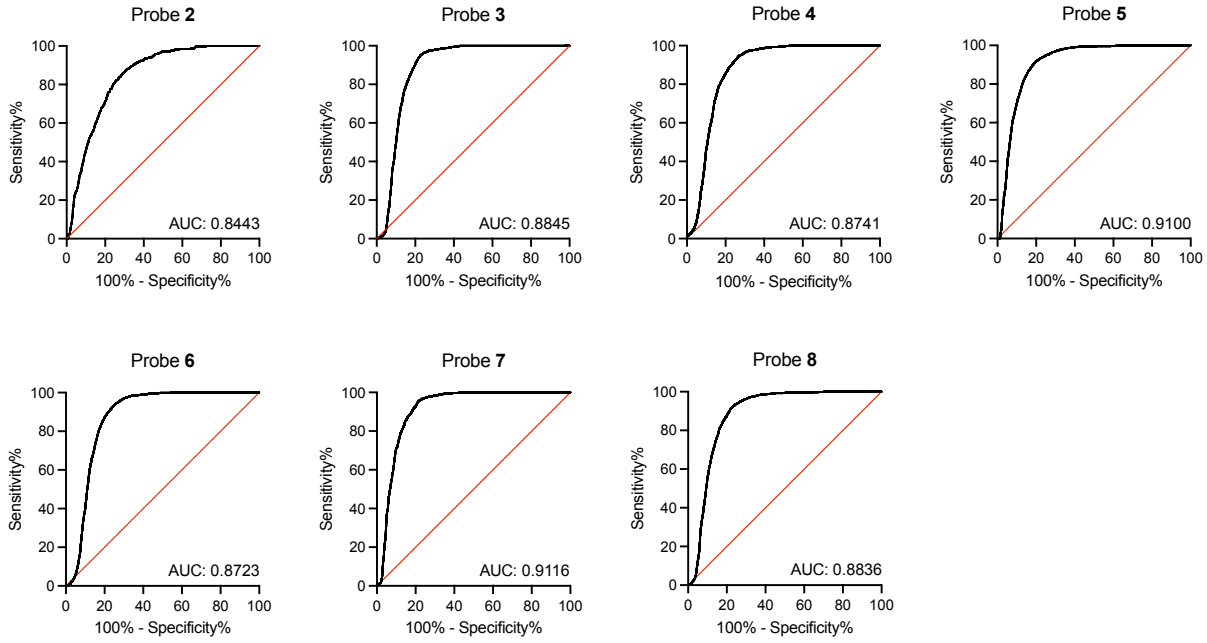

Supplementary Figure 6. Retention time ROC curves for probes **2**-**8**.

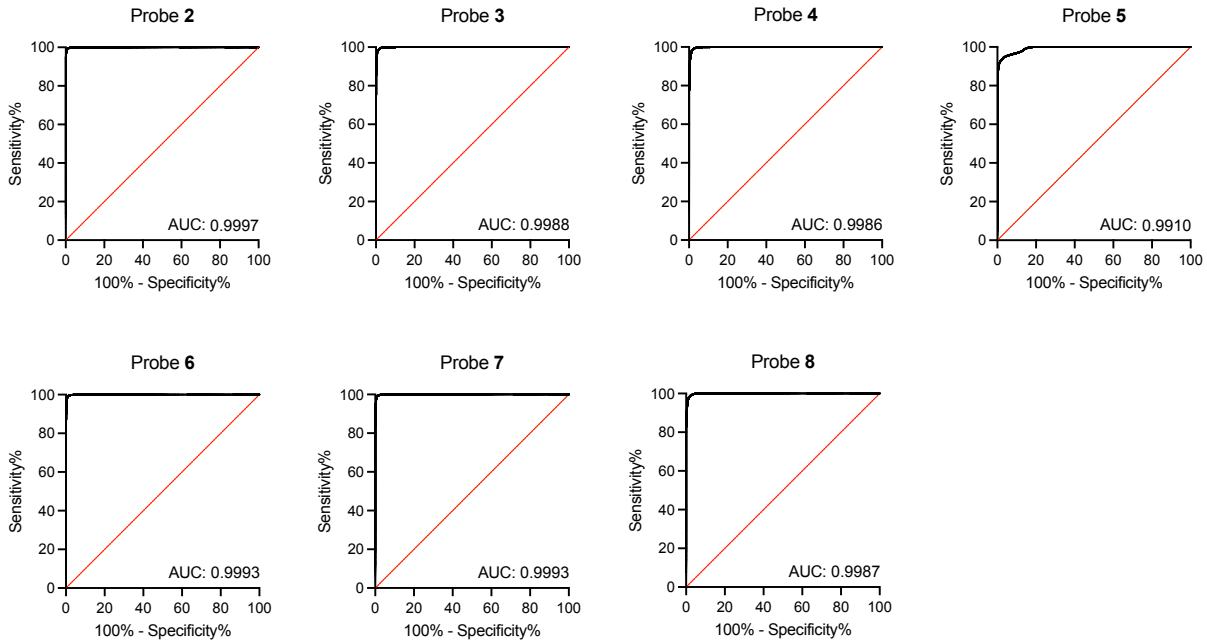

Supplementary Figure 7. Final model ROC curves for probes **2**-**8**.

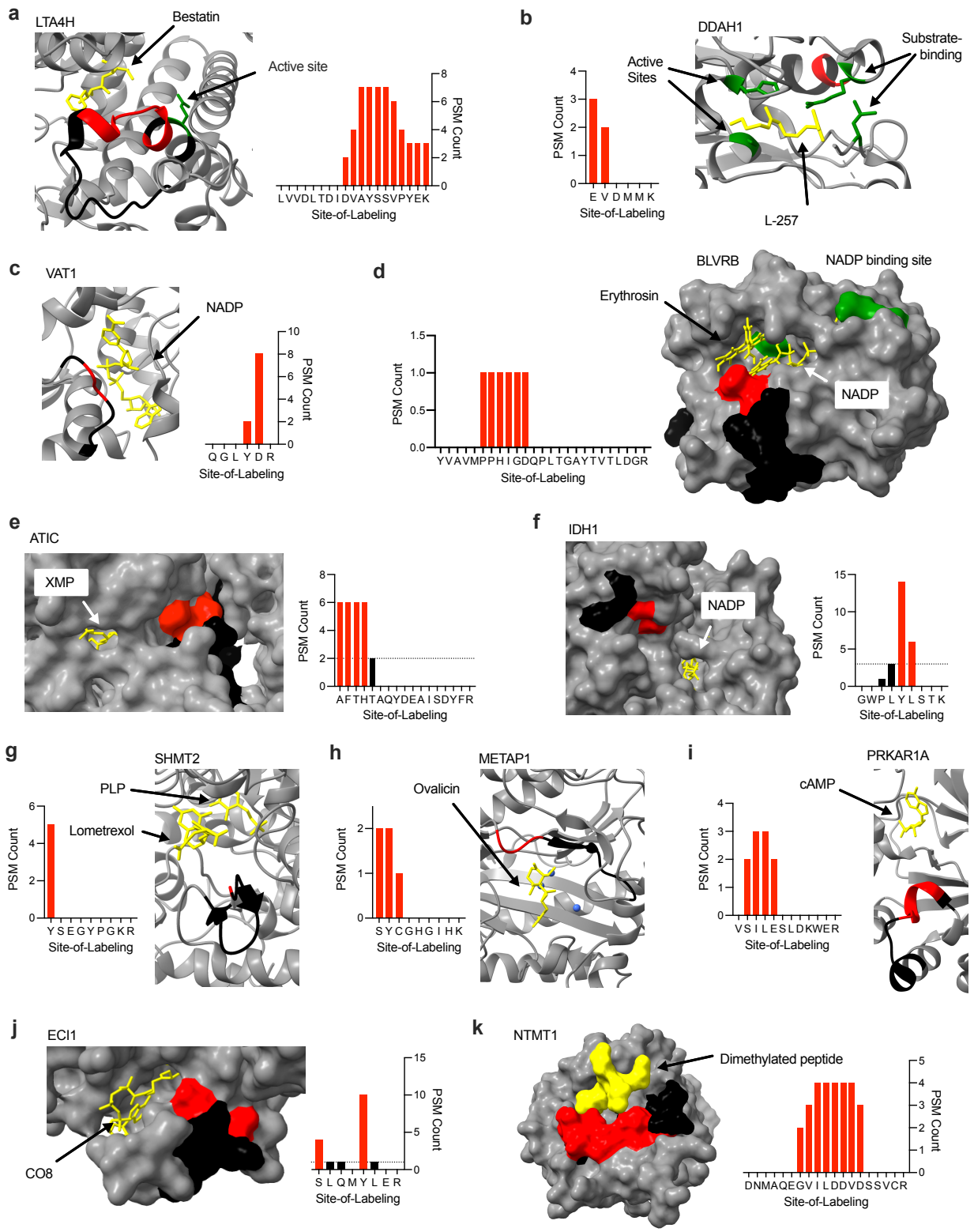

Supplementary Figure 8. Additional examples of labeling events mapped to PDB structures. For all structures, labeled peptide residues are colored red and the remainder of each peptide is colored black. Active/other indicated sites are colored green and co-resolved ligands are colored yellow. (**a**) LTA4H probe label site overlapping with active site inhibitor Bestatin (PDB: 1HS6). (**b**)

DDAH1 probe label site overlapping with active site inhibitor L-257 (PDB: 2JAJ). (**c**) VAT1 probe label site overlapping with NADP binding site (PDB: 6LHR). (**d**) BLVRB probe label site overlapping with erythrosine binding site (PDB: 5OOH). (**e**) ATIC probe label site overlapping with XMP binding site (PDB: 1PKX). (**f**) IDH1 probe label site overlapping with NADP binding site (PDB: 1T0L). (**g**) SHMT2 probe label site overlapping with lometrexol and pyridoxal-5'-phosphate (PLP) binding site (PDB: 6QVG). (**h**) METAP1 probe label site overlapping with ovalicin binding site (PDB: 2GZ5). (**i**) PRKAR1A probe label site overlapping with cAMP binding site (PDB: 5KJX). (**j**) ECI1 probe label site overlapping with CO8 binding site (PDB: 1SG4). (**k**) NTMT1 probe label site overlapping with dimethylated peptide binding site (PDB: 5CVD).

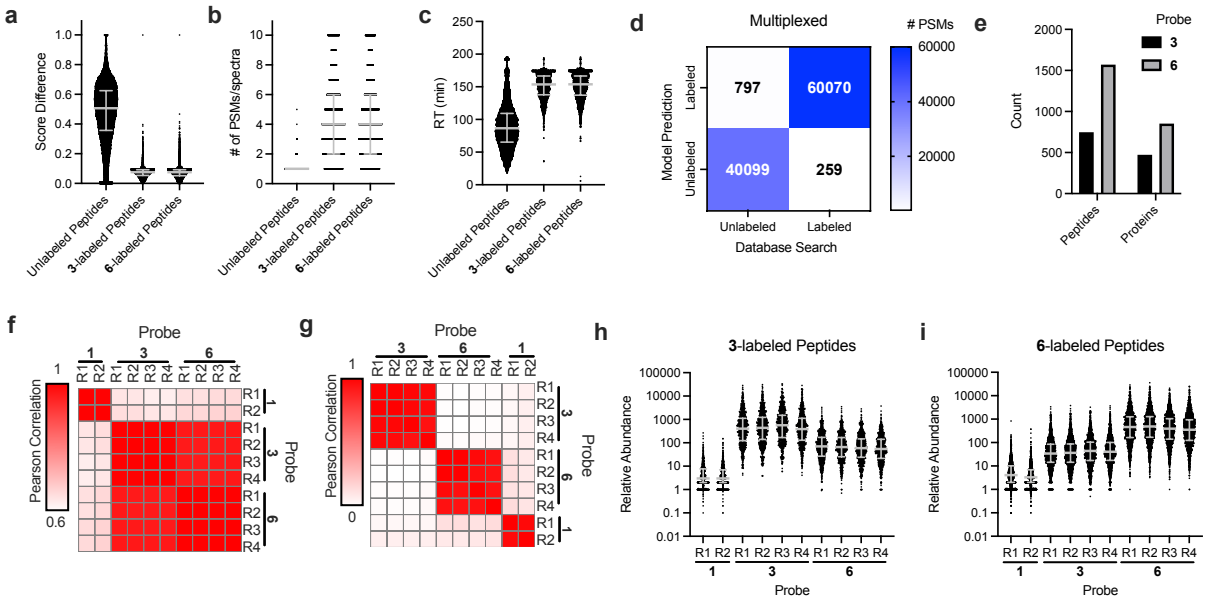

Supplementary Figure 9. Extended proteomic data for TMT SoL pilot experiment. (**a**) Score differences between first and second ranked PSMs for spectra assigned to labeled and unlabeled peptides. (**b**) Number of PSMs assigned to spectra containing labeled and unlabeled peptides. (**c**) Retention time of spectra assigned to labeled and unlabeled peptides. For a-c, error bars were calculated from n = 40,333 (unlabeled), n = 4889 (**3**-labeled) and n = 9014 (**6**-labeled) PSMs. (**d**) Confusion matrix for model built in in Figure 3 applied to multiplexed data. (**e**) Numbers of probe-labeled peptides and proteins detected in multiplexed experiments by each probe. (**f**) Correlation of TMT quantitation from whole protein enrichment samples. (**g**) Correlation of TMT quantitation from SoL samples. (**h-i**) Relative TMT abundance for all probe **3**-labeled peptides (**h**) and probe **6**-labeled peptides (**i**). For h-i, error bars were calculated for n = 799 unique peptides. Error bars for all plots represent the median -/+ the interquartile range.

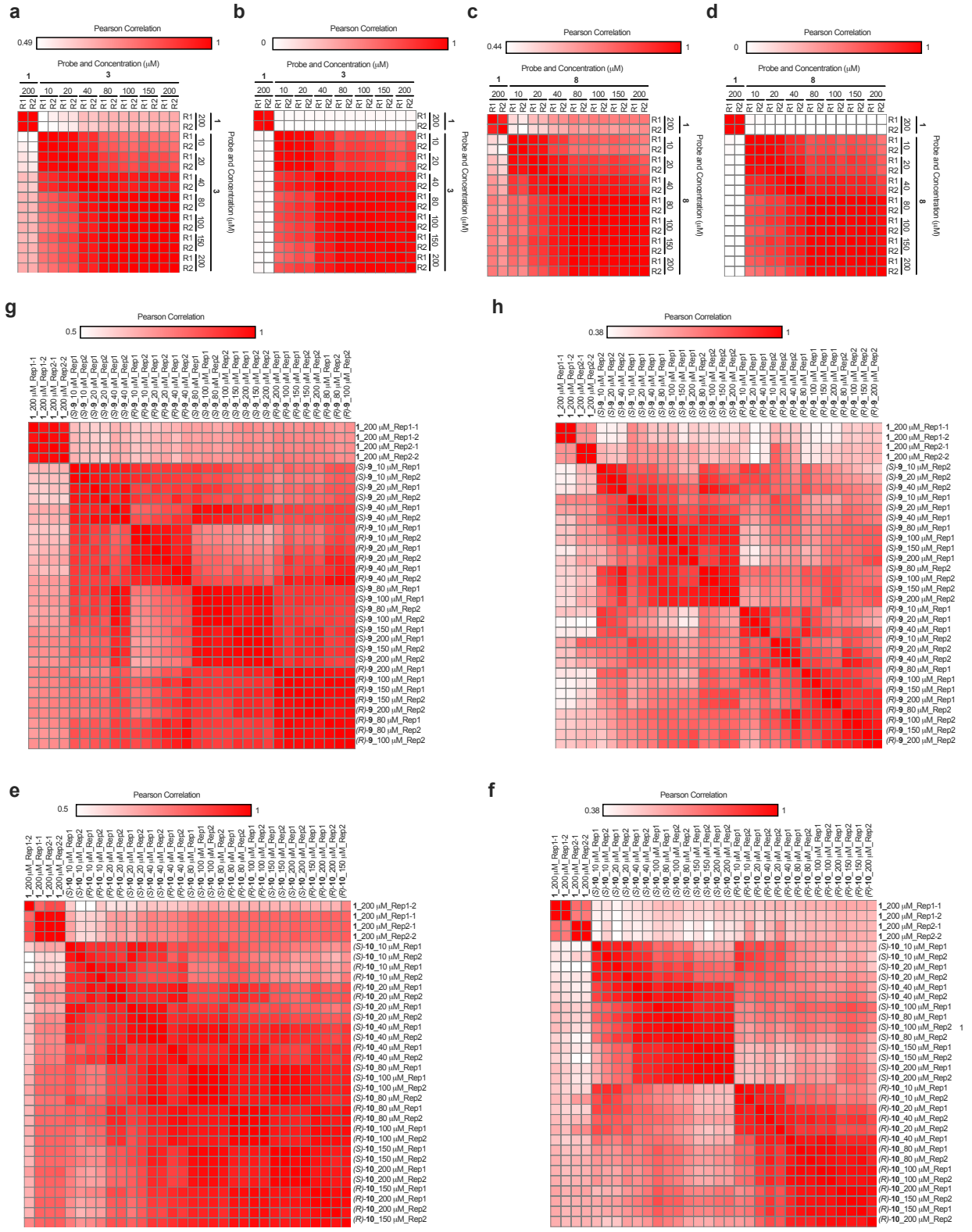

Supplementary Figure 10. Correlation matrices from TMT dose SoL experiments. Correlation of TMT quantitation from probe **3** whole protein samples (**a**) and SoL samples (**b**). Correlation of TMT quantitation from probe **8** whole protein samples (**c**) and SoL samples (**d**). Correlation of

TMT quantitation from *(R)/(S)*-**9** whole protein samples (**g**) and SoL samples (**h**). Correlation of TMT quantitation from *(R)/(S)*-**10** whole protein samples (**e**) and SoL samples (**f**).

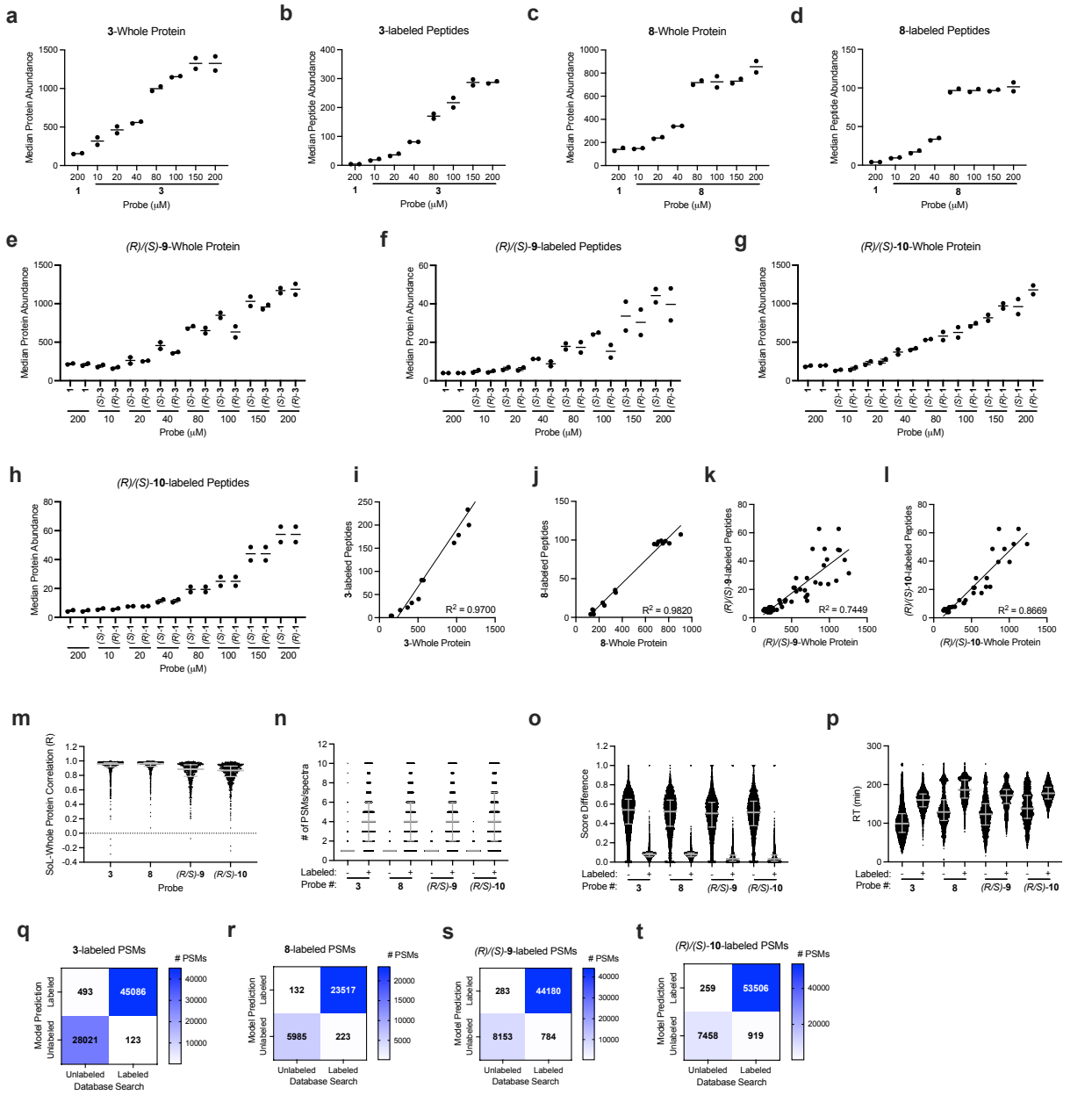

Supplementary Figure 11. Supplementary proteomic data for TMT dose SoL experiments. Median abundances from probe **3** whole protein samples (**a**) and SoL samples (**b**). Median abundances from probe **8** whole protein samples (**c**) and SoL samples (**d**). Median abundances from probe *(R)/(S)*-**9** whole protein samples (**e**) and SoL samples (**f**). Median abundances from probe *(R)/(S)*-**10** whole protein samples (**g**) and SoL samples (**h**). Correlation of whole protein and SoL channel medians for probe **3** (**i**), probe **8** (**j**), probes *(R)/(S)*-**9** (**k**) and probes *(R)/(S)*-**10** (**l**). (**m**) Correlation of SoL peptide quantitation with respective whole protein quantitation. Error bars were calculated from n = 1420 (**3**), n = 1047 (**8**), n = 695 (*(R)/(S)*-**9**), and n = 889 (*(R)/(S)*-**10**) peptide-protein pairs. (**n**) Number of PSMs assigned to spectra containing labeled and unlabeled peptides. (**o**) Score differences between first and second ranked PSMs for spectra assigned to labeled and unlabeled peptides. (**p**) Retention time of spectra assigned to labeled and unlabeled peptides. For n-p, error bars were calculated from n = 28,021 (**3**-unlabeled), n = 10,508 (**3**-labeled), n = 5976 (**6**-unlabeled), n = 6003 (**6**-labeled), n = 8290 (*(R)/(S)*-**9**-unlabeled),

n = 10,155 (*(R)/(S)*-**9**-labeled), n = 7587 (*(R)/(S)*-**10**-unlabeled), and n = 12,243 (*(R)/(S)*-**10**-labeled) PSMs. Confusion matrix for model built in Figure 3 applied to multiplexed data for probe **3** (**q**), probe **8** (**r**), probes *(R)/(S)*-**9** (**s**) and probes *(R)/(S)*-**10** (**t**). Error bars for all plots represent the median -/+ the interquartile range.

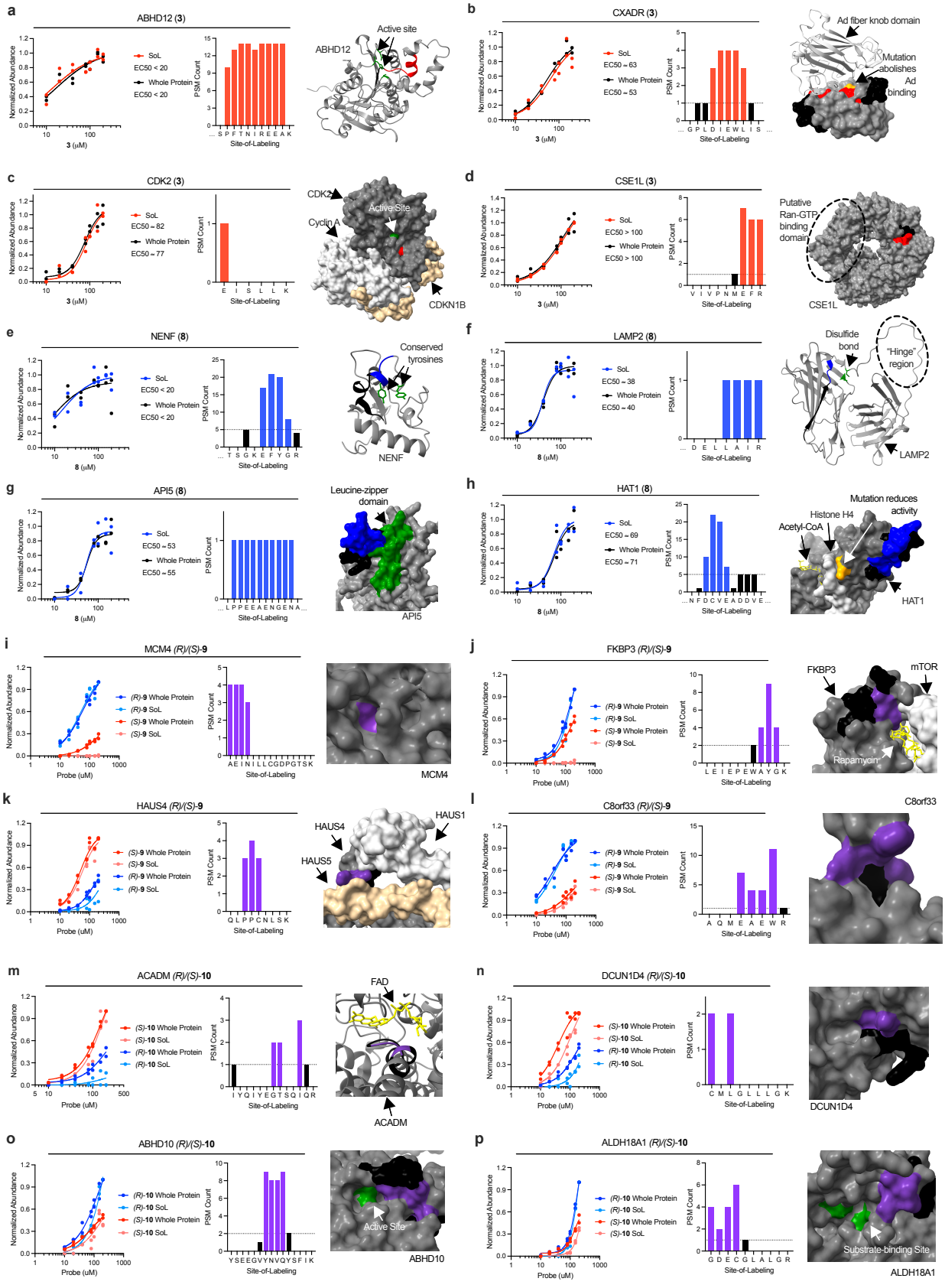
a
ABHD12 (3)
SoL
EC50 < 20
Whole Protein
EC50 < 20
Normalized Abundance
3 (μM)
PSM Count
Site-of-Labeling
S P F T N I R E E A K
ABHD12
Active site
b
CXADR (3)
SoL
EC50 ~ 63
Whole Protein
EC50 ~ 53
G P L D I E W L I S
Ad fiber knob domain
Mutation abolishes Ad binding
c
CDK2 (3)
SoL
EC50 ~ 82
Whole Protein
EC50 ~ 77
E I S L L K
CDK2
Cyclin A
Active Site
CDKN1B
d
CSE1L (3)
SoL
EC50 > 100
Whole Protein
EC50 > 100
V I V P N M E F R
Putative Ran-GTP binding domain
CSE1L
e
NENF (8)
SoL
EC50 < 20
Whole Protein
EC50 < 20
8 (μM)
T S G K E F Y G R
Conserved tyrosines
NENF
f
LAMP2 (8)
SoL
EC50 ~ 38
Whole Protein
EC50 ~ 40
D E L L A I R
Disulfide bond
"Hinge" region
LAMP2
g
API5 (8)
SoL
EC50 ~ 53
Whole Protein
EC50 ~ 55
L P P E E A E N G E N A
Leucine-zipper domain
API5
h
HAT1 (8)
SoL
EC50 ~ 69
Whole Protein
EC50 ~ 71
N F D C V E A D D V E
Mutation reduces activity
Histone H4
Acetyl-CoA
HAT1
i
MCM4 (R)/(S)-9
(R)-9 Whole Protein
(R)-9 SoL
(S)-9 Whole Protein
(S)-9 SoL
Probe (uM)
A E I N I L L C G D P G T S K
MCM4
j
FKBP3 (R)/(S)-9
L E I E P E W A Y G K
FKBP3
mTOR
Rapamycin
k
HAUS4 (R)/(S)-9
Q L P P C N L S K
HAUS4
HAUS1
HAUS5
l
C8orf33 (R)/(S)-9
A Q M E A E W R
C8orf33
m
ACADM (R)/(S)-10
(S)-10 Whole Protein
(S)-10 SoL
(R)-10 Whole Protein
(R)-10 SoL
I Y Q I Y E G T S Q I Q R
FAD
ACADM
n
DCUN1D4 (R)/(S)-10
C M L G L L L G K
DCUN1D4
o
ABHD10 (R)/(S)-10
Y S E E G V Y N V Q Y S F I K
Active Site
ABHD10
p
ALDH18A1 (R)/(S)-10
G D E C G L A L G R
Substrate-binding Site
ALDH18A1

Supplementary Figure 12. Examples of proteome-wide, site-specific, concentration-dependent probe-protein interaction profiles. For all structures, peptide residues labeled by probes are colored red (for probe **3**), blue (for probe **8**) or purple (for stereochemically matched probe pairs) and the remainder of each peptide is colored black. Active/other indicated sites are colored green and functional mutation sites are colored orange. (**a**) ABHD12 concentration plot and probe label site proximal to active site (AF-Q8N2K0-F1-model_v2). (**b**) CXADR concentration plot and probe label site overlapping to Ad12 fiber knob domain binding site (PDB: 1KAC). (**c**) CDK2 concentration plot and probe label site overlapping active site (PDB: 6ATH). (**d**) CSE1L concentration plot and probe label site proximal to putative Ran-GTP binding domain (AF-P55060-F1-model_v2). (**e**) NENF concentration plot and probe label site in the heme-binding domain (AF-Q9UMX5-F1-model_v2). (**f**) LAMP2 concentration plot and probe label site proximal to disulfide bond and “hinge” region (AF-P13473-F1-model_v2). (**g**) API5 concentration plot and probe label site proximal to leucine-zipper domain (AF-Q9BZZ5-F1-model_v2). (**h**) HAT1 concentration plot and probe label site (PBD: 2P0W). (**i**) MCM4 concentration plot and probe label site proximal to clear pocket (PDB: 6XTX). (**j**) FKBP3 concentration plot and probe label site proximal to rapamycin binding site in complex with mTOR (PDB: 5GPG). (**k**) HAUS4 concentration plot and probe label site proximal to PPI with HAUS1 and HAUS5 (PDB: 7SQK). (**l**) C8orf33 concentration plot and probe label site proximal to clear pocket (AF-Q9H7E9-F1-model_v2). (**m**) ACADM concentration plot and probe label site proximal to FAD binding site (PBD: 1EGE). (**n**) DCUN1D4 concentration plot and probe label site proximal to clear pocket (AF-Q92564-F1-model_v2). (**o**) ABHD10 concentration plot and probe label site proximal to active site (AF-Q9NUJ1-F1-model_v2). (**p**) ALDH18A1 concentration plot and probe label site proximal to active site (AF-P54886-F1-model_v2). All calculated EC50 values are approximations.

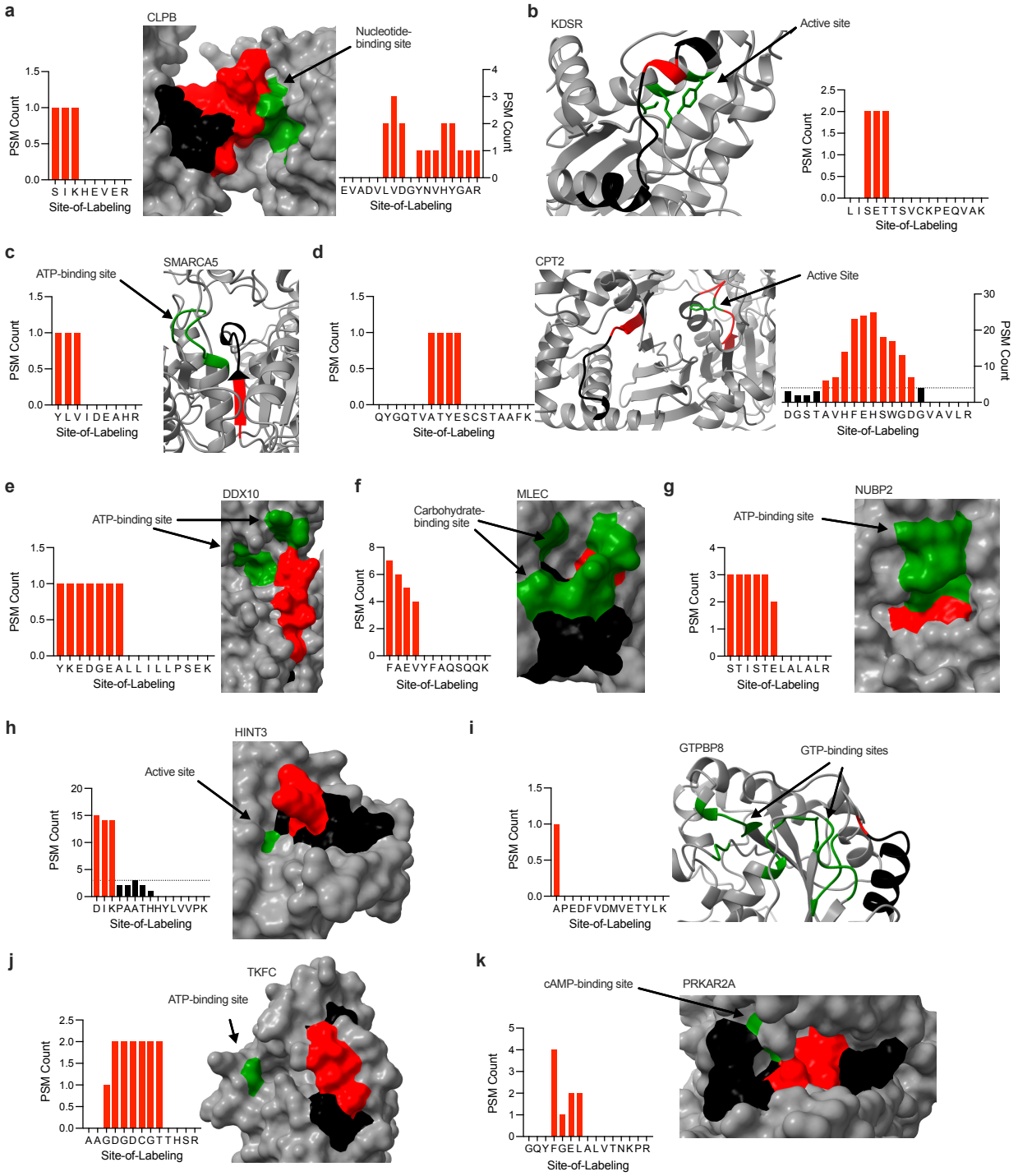

Supplementary Figure 13. Examples of labeling events mapped to Alpha Fold structures. For all structures, labeled peptide residues are colored red and the remainder of each peptide is colored black. Active/other indicated sites are colored green. (**a**) CLPB probe label site overlapping with nucleotide binding site (AF-Q9H078-F1-model_v2). (**b**) KDSR probe label site overlapping with active site (AF-Q06136-F1-model_v2). (**c**) SMARCA5 probe label site overlapping with ATP-binding site (AF-O60264-F1-model_v2). (**d**) CPT2 probe label site overlapping with active site (AF-P23786-F1-model_v2). (**e**) DDX10 probe label site overlapping with ATP-binding site (AF-Q13206-F1-model_v2). (**f**) MLEC probe label site overlapping with

carbohydrate binding site (AF-Q14165-F1-model_v2). (**g**) NUBP2 probe label site overlapping with ATP-binding site (AF-Q9Y5Y2-F1-model_v2). (**h**) HINT3 probe label site overlapping with active site (AF-Q9NQE9-F1-model_v2). (**i**) GTPBP8 probe label site overlapping with GTP binding site (AF-Q8N3Z3-F1-model_v2). (**j**) TKFC probe label site overlapping with ATP-binding site (AF-Q3LXA3-F1-model_v2). (**k**) PRKAR2A probe label site overlapping with cAMP binding site (AF-P13861-F1-model_v2).

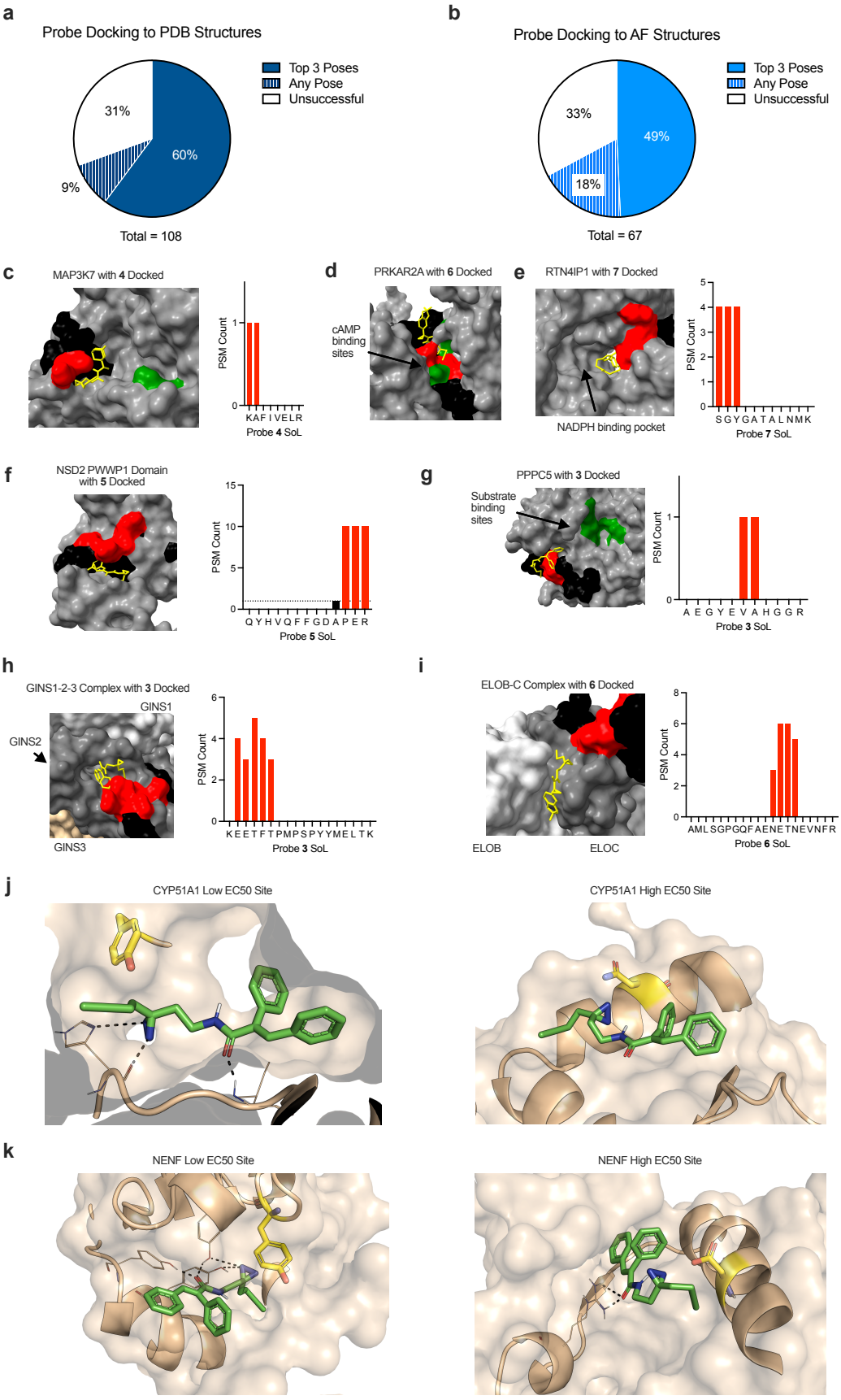
a
Probe Docking to PDB Structures
Top 3 Poses
Any Pose
Unsuccessful
31%
60%
9%
Total = 108
b
Probe Docking to AF Structures
Top 3 Poses
Any Pose
Unsuccessful
33%
49%
18%
Total = 67
c
MAP3K7 with 4 Docked
PSM Count
KAF I VELR
Probe 4 SoL
d
PRKAR2A with 6 Docked
cAMP binding sites
e
RTN4IP1 with 7 Docked
NADPH binding pocket
PSM Count
S G Y G A T A L N M K
Probe 7 SoL
f
NSD2 PWWP1 Domain with 5 Docked
PSM Count
Q Y H V Q F F G D A P E R
Probe 5 SoL
g
PPPC5 with 3 Docked
Substrate binding sites
PSM Count
A E G Y E V A H G G R
Probe 3 SoL
h
GINS1-2-3 Complex with 3 Docked
GINS1
GINS2
GINS3
PSM Count
K E E T F T P M P S P Y Y M E L T K
Probe 3 SoL
i
ELOB-C Complex with 6 Docked
ELOB
ELOC
PSM Count
A M L S G P G Q F A E N E T N E V N F R
Probe 6 SoL
j
CYP51A1 Low EC50 Site
CYP51A1 High EC50 Site
k
NENF Low EC50 Site
NENF High EC50 Site

Supplementary Figure 14. Docking analysis of diverse sites. (**a**) Success rate of probe docking to PDB structures. (**b**) Success rate of probe docking to AF structures. (**c** - **i**) Depictions of docked low-energy binding modes consistent with adducted residues detected via proteomics for MAP3K7 (**c**; 5GJF), PRKAR2A (**d**; AF-P13861-F1-model_v2), RTN4IP1 (**e**; 2VN8), NSD2 (**f**; 6XCG), PPPC5 (**g**; 1S95), GINS2 (**h**; 2E9X), ELOC (**i**; 6I7R), For all structures, labeled peptide residues are colored red and the remainder of each detected peptide is colored black. Docked probes are colored yellow. Active/other indicated sites are colored green and overlay detected peptide residues where appropriate. All panels except d also contain corresponding peptide plots. The peptide plot for panel d is depicted in Supplementary Fig. 13k. (**j** - **k**) Detailed docking analysis of probe **3** low and high EC50 sites for CYP51A1 (**j**; 6Q2T) and NENF (**k**; AF-Q9UMX5-F1-model_v2). For detailed docking figures, docked probes are colored green, the closest labeled residue to the diazirine moiety is colored yellow and predicted hydrogen bonds are depicted as black dashed lines.

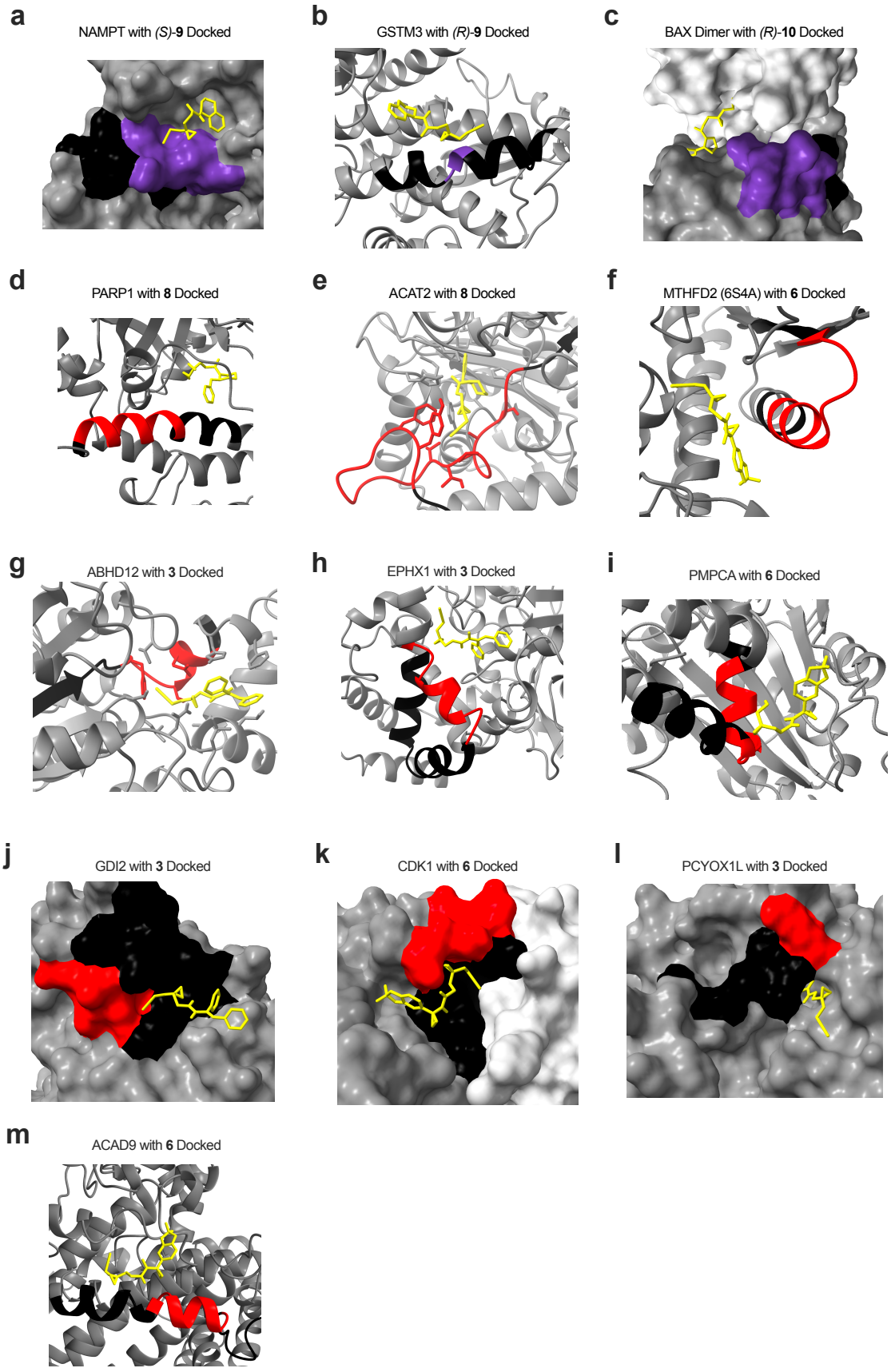
a
NAMPT with (S)-9 Docked
b
GSTM3 with (R)-9 Docked
c
BAX Dimer with (R)-10 Docked
d
PARP1 with 8 Docked
e
ACAT2 with 8 Docked
f
MTHFD2 (6S4A) with 6 Docked
g
ABHD12 with 3 Docked
h
EPHX1 with 3 Docked
i
PMPCA with 6 Docked
j
GDI2 with 3 Docked
k
CDK1 with 6 Docked
l
PCYOX1L with 3 Docked
m
ACAD9 with 6 Docked

Supplementary Figure 15. Docking analysis of validated probe-protein interactions. Depictions of docked low-energy binding modes consistent with adducted residues detected via proteomics for NAMPT (**a**; PDB: 4KFN), GSTM3 (**b**; 3GTU), BAX (**c**; 4S0O), PARP1 (**d**; 7KK4), ACAT2 (**e**; 1WL5), MTHFD2 (**f**; 6S4A), ABHD12 (**g**; AF-Q8N2K0-F1-model_v2), EPHX1 (**h**; AF-P07099-F1-model_v2), PMPCA (**i**; AF-Q10713-F1-model_v2), GDI2 (**j**; AF-P50395-F1-model_v2), CDK1 (**k**; 4Y72), PCYOX1L (**l**; AF-Q8NBM8-F1-model_v2), and ACAD9 (**m**; AF-Q9H845-F1-model_v2). For all structures, labeled peptide residues are colored purple (for stereochemically matched probe pairs) or red (for standard probes) and the remainder of each detected peptide is colored black. Docked probes are colored yellow. Active/other indicated sites are colored green and overlay detected peptide residues where appropriate. Corresponding peptide plots are depicted in previous figures (Fig. 5 for a, c; Extended Data Fig. 4 for b, Fig. 6 for d and j-k; Extended Data Fig. 7 for e-f, Supplementary Fig. 12 for g, Extended Data Fig. 8 for i and l-m).

Supplementary Notes

Supplementary Note 1. Comparison of multiPSM search to ptmRS localization.

Several computational tools already exist to aid in the localization of post translational modifications (PTMs) on peptide sequences. In theory, these approaches can be applied to any type of modification (eg. phosphorylation, acetylation, etc.). To explore the utility of such approaches in localizing photoaffinity probe modifications, we analyzed our data using the ptmRS algorithm[1], a standard tool for assigning confidence to modification positions and compared the results to the multiPSM approach described in the main text. We found that the approaches largely agreed on a subset of sites (**Extended Data Fig. 1a**), but the multiPSM search reported thousands more unique labeling events compared to ptmRS. Further investigation revealed numerous cases where ptmRS incorrectly assigned a single label site to a peptide where multiple positions were clearly supported in the fragment spectra (example shown in **Extended Data Fig. 1b-c**). Furthermore, for the same peptide in the same experiment, ptmRS calls multiple different probe locations with >98% confidence that just a single site is labeled. Together, this suggests that ptmRS is suboptimal for localizing the unique modification patterns generated from photoaffinity probes, perhaps because such tools were developed to localize relatively sparse endogenous modifications on specific amino acid residues and validated on synthetic peptides with known modification positions[1-4]. Due to this limitation, the remainder of the analyses are performed on the multiPSM search results; albeit with the caveat that no FDR is reported for site assignments due to the complexity of having multiple peptides identified from the same spectrum.

Supplementary Note 2. Compound synthesis and characterization

Materials

Chemicals and reagents were purchased from commercial vendors, including Sigma-Aldrich, Fisher Scientific, Combi-Blocks, MedChemExpress, Alfa Aesar and AstaTech, and were used as received without further purification, unless otherwise noted. Anhydrous solvents were purchased from Sigma-Aldrich in Sure/Seal™ formulations. All reactions were monitored by thin-layer chromatography (TLC, Merck silica gel 60 F-254 plates). The plates were stained either with p-anisaldehyde (2.5% p-anisaldehyde, 1% AcOH, 3.5% H_2SO_4 (conc.) in 95% EtOH), ninhydrin (0.3% ninhydrin (w/v), 97:3 EtOH-AcOH), $KMnO_4$ (1.5 g of $KMnO_4$, 10 g K_2CO_3, and 1.25 ml 10% NaOH in 200 ml water), iodine or directly visualized with UV light. Reaction purification was carried out using Flash chromatography (230 – 400 mesh silica gel), Biotage® or preparative thin layer chromatography (PTLC, Analtech, 500 – 2000 µm thickness). NMR spectra were recorded on

Bruker DPX-400 or Bruker AV-500 spectrometers in the indicated solvent. Multiplicities are reported with the following abbreviations: s singlet; d doublet; t triplet; q quartet; p pentet; m multiplet; br broad; dd doublet of doublets; dt doublet of triplets; td triplet of doublets; Chemical shifts are reported in ppm relative to the residual solvent peak and J values are reported in Hz. Mass spectrometry data were collected on an Agilent 6120 single-quadrupole LC/MS instrument (ESI, low resolution) or an Agilent ESI-TOF instrument (ESI-TOF, high resolution).

General synthetic procedure of diazirine containing probe:

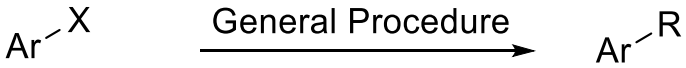

X = COOH, NH_2

General Procedure 1: To a solution of corresponding commercially available carboxylic acid (0.113 mmol) in 3 ml DCM, the corresponding diazirine amine (0.118 mmol), DIPEA (0.354 mmol), EDC-HCl (0.177 mmol), and HOBt (0.177 mmol) were added. The reaction mixtures were stirred at room temperature for 14 to 16 hr. After completion (monitored by TLC) the crude reaction mixture was diluted with DCM (20 ml) and washed first with saturated aqueous NH_4Cl (10 ml) and saturated aqueous $NaHCO_3$ (10 ml) solution, dried over anhydrous Na_2SO_4 and volatiles removed by rotary evaporation. Crude products were purified by PTLC or Biotage® SNAP Cartridge KP-Sil Snap 10 g with linear gradient of ethyl acetate and hexane over 20 column volumes (CV).

General Procedure 2: To a solution of corresponding commercially available amine (0.113 mmol) in 3 ml DMF, the corresponding diazirine acid (0.118 mmol), DIPEA (0.354 mmol), and HATU (0.177 mmol) were added. The reaction mixtures were stirred cooling at 0 °C for 10 min. After completion (monitored by TLC) the crude reaction mixture was diluted with ethyl acetate (20 ml) and washed first with saturated aqueous NH_4Cl (10 ml) and saturated aqueous $NaHCO_3$ (10 ml) solution, dried over anhydrous Na_2SO_4 and volatiles removed by rotary evaporation. Crude products were purified by PTLC or Biotage® SNAP Cartridge, KP-Sil, 10 g with linear gradient of ethyl acetate and hexane over 20 CVs.

Characterization data of fully functionalized fragment (FFF) probes:

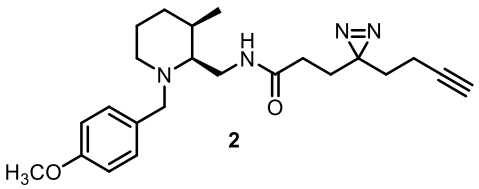

2

rac-3-(3-(but-3-yn-1-yl)-3H-diazirin-3-yl)-N-(((2S,3R)-1-(4-methoxybenzyl)-3-methylpiperidin-2-yl)methyl)propanamide (2): Synthesized according to general procedure 2. The residue obtained was purified by Biotage® (Hexanes/EtOAc, 8:2) to afford **2** as a colorless liquid (13 mg, 62%). ^{1}H NMR (400 MHz, CDCl3) δ 7.20 (d, J = 8.2 Hz, 2H), 6.92 – 6.86 (m, 2H), 6.24 – 6.11 (m, 1H), 3.82 (s, 3H), 3.76 (s, 2H), 3.43 – 3.31 (m, 1H), 3.14 – 3.09 (m, 1H), 2.79 – 2.69 (m, 1H), 2.67 – 2.50 (m, 2H), 2.12 – 2.06 (m, 1H), 2.06 – 1.97 (m, 3H), 1.92 – 1.72 (m, 5H), 1.68 – 1.56 (m, 3H), 1.37 – 1.27 (m, 2H), 0.86 – 0.79 (m, 3H). ^{13}C NMR (126 MHz, CDCl3) δ 170.95, 158.85, 132.01, 129.88, 129.78, 113.86, 82.71, 69.07, 58.91, 56.73, 55.24, 45.07, 32.37, 30.55, 29.71, 28.59, 27.91, 27.02, 20.54, 18.15, 13.32. HRMS (ESI-TOF) *calcd for* $C_{23}H_{33}N_4O_2$, 397.5425 ($M+H^+$), found 397.2549.

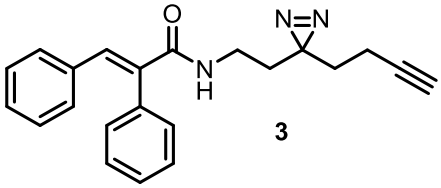

3

(E)-N-(2-(3-(but-3-yn-1-yl)-3H-diazirin-3-yl)ethyl)-2,3-diphenylacrylamide (3): Synthesized according to general procedure 1, purified by Biotage® (Hexanes/EtOAc, 7:3) to afford **3** as a colorless liquid (16 mg, 74%).^{1}H NMR (500 MHz, $CDCl_3$) δ 7.85 (s, 1H), 7.49 – 7.42 (m, 3H), 7.32 – 7.27 (m, 2H), 7.20 – 7.10 (m, 3H), 6.99 (dd, J = 7.5, 1.8 Hz, 2H), 5.59 (t, J = 6.0 Hz, 1H), 3.18 (q, J = 6.5 Hz, 2H), 1.95 (td, J = 7.4, 2.7 Hz, 2H), 1.91 (t, J = 2.7 Hz, 1H), 1.66 (t, J = 6.7 Hz, 2H), 1.59 (t, J = 7.4 Hz, 2H). ^{13}C NMR (126 MHz, $CDCl_3$) δ 167.06, 137.32, 136.04, 134.87, 134.12, 130.42, 129.93, 129.71, 128.66, 128.63, 128.17, 82.56, 69.29, 35.02, 32.54, 32.14, 26.73, 13.16. HRMS (ESI-TOF) *calcd for* $C_{22}H_{22}N_3O$, 344.1757 ($M+H^+$), *found* 344.1734.

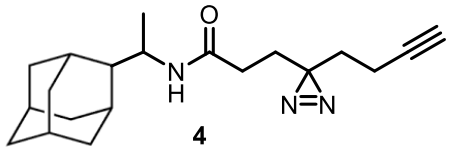

4

N-(1-((3,5,7)-adamantan-1-yl)ethyl)-3-(3-(but-3-yn-1-yl)-3H-diazirin-3-yl)propanamide (4): Synthesized according to general procedure 2, purified by Biotage® (Hexanes/EtOAc, 8:2) to afford **4** as a white solid (11 mg, 67%). ^{1}H NMR (400 MHz, $CDCl_3$) δ 5.26 (d, J = 9.8 Hz, 1H), 3.74 – 3.67 (m, 1H), 2.06 – 1.96 (m, 6H), 1.97 – 1.81 (m, 4H), 1.76 – 1.58 (m, 8H), 1.58 – 1.43 (m, 6H), 1.06 – 0.98 (m, 3H). ^{13}C NMR (151 MHz, $CDCl_3$) δ 170.76, 83.08, 69.52, 53.41, 38.73, 37.37, 36.07, 32.82, 31.03, 28.82, 28.63, 28.27, 14.89, 13.67.

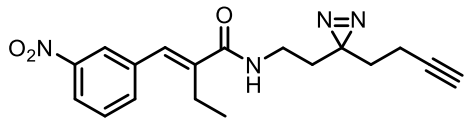

5

(E)-N-(2-(3-(but-3-yn-1-yl)-3H-diazirin-3-yl)ethyl)-2-(3-nitrobenzylidene)butanamide (5): Synthesized according to general procedure 1, purified by Biotage® (Hexanes/EtOAc, 7:3) to afford **5** as a light-yellow solid (14 mg, 76%). ^{1}H NMR (400 MHz, $CDCl_3$) δ 8.16 – 8.08 (m, 2H), 7.63 – 7.48 (m, 2H), 7.15 (s, 1H), 6.24 (t, J = 5.9 Hz, 1H), 3.23 (q, J = 6.4 Hz, 2H), 2.50 (q, J = 7.5 Hz, 2H), 2.06 – 1.96 (m, 3H), 1.78 (t, J = 6.6 Hz, 2H), 1.67 (t, J = 7.1 Hz, 2H), 1.14 (t, J = 7.5 Hz, 3H). ^{13}C NMR (151 MHz, $CDCl_3$) δ 168.97, 148.32, 142.44, 137.70, 134.84, 129.71, 129.58, 123.59, 122.63, 82.77, 69.53, 34.94, 32.43, 32.11, 27.00, 21.29, 13.39, 13.27. HRMS (ESI-TOF) *calcd for* $C_{18}H_{21}N_4O_3$, 341.1608 ($M+H^+$), *found* 341.1612.

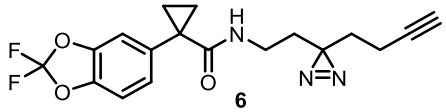

6

N-(2-(3-(but-3-yn-1-yl)-3H-diazirin-3-yl)ethyl)-1-(2,2-difluorobenzo[d][1,3]dioxol-5-yl)cyclopropane-1-carboxamide (6): Synthesized according to general procedure 1, purified by Biotage® (Hexanes/EtOAc, 6:4) to afford **6** as a white solid (15 mg, 78%).^{1}H NMR (500 MHz, $CDCl_3$) δ 7.23 – 7.16 (m, 2H), 7.09 (d, J = 8.1 Hz, 1H), 5.39 (d, J = 6.2 Hz, 1H), 3.08 (q, J = 6.4 Hz, 2H), 2.00 – 1.93 (m, 3H), 1.60 (m, 6H), 1.05 (q, J = 3.8 Hz, 2H). ^{13}C NMR (126 MHz, $CDCl_3$) δ 173.24, 144.12, 143.51, 135.90, 131.80 (t, J = 256.0 Hz), 126.63, 112.50, 109.95, 82.65, 69.34, 35.26, 32.63, 32.13, 30.46, 26.84, 16.14, 16.12, 13.17. HRMS (ESI-TOF) *calcd for* $C_{18}H_{18}F_2N_3O_3$, 362.1311 ($M+H^+$), *found* 362.1312.

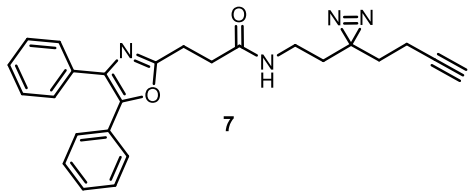

7

N-(2-(3-(but-3-yn-1-yl)-3H-diazirin-3-yl)ethyl)-3-(4,5-diphenyloxazol-2-yl)propanamide (7): Synthesized according to general procedure 1, purified by Biotage® (Hexanes/EtOAc, 6:4) to afford **7** as a white solid (14 mg, 72%).^{1}H NMR (400 MHz, $CDCl_3$) δ 7.64 – 7.60 (m, 2H), 7.59 – 7.55 (m, 2H), 7.40 – 7.31 (m, 6H), 6.18 (s, 1H), 3.21 (t, J = 7.2 Hz, 2H), 3.13 (td, J = 6.7, 5.8 Hz, 2H), 2.78 (t, J = 7.2 Hz, 2H), 2.01 – 1.93 (m, 3H), 1.67 (t, J = 6.8 Hz, 2H), 1.58 (s, 2H). ^{13}C NMR

(151 MHz, $CDCl_3$) δ 171.44, 162.43, 145.57, 134.97, 132.44, 128.89, 128.73, 128.67, 128.60, 128.22, 127.94, 126.52, 82.76, 69.49, 34.47, 33.04, 32.52, 32.12, 26.84, 24.00, 13.26. HRMS (ESI-TOF) *calcd for* $C_{25}H_{25}N_4O_2$, 413.1972 ($M+H^+$), *found* 413.1947.

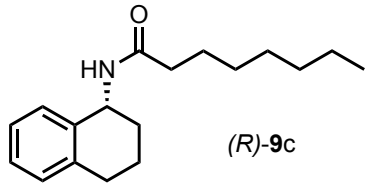

(R)-**9**c

(R)-N-(1,2,3,4-tetrahydronaphthalen-1-yl)octanamide (R9c): Synthesized according to general procedure 1. The residue obtained was purified by Biotage® (Hexanes/EtOAc, 7:3) to afford **R9c** as a colorless liquid (15.3 mg, 73%). ^1H NMR (600 MHz, $CDCl_3$) δ 7.28 – 7.24 (m, 1H), 7.18 (dd, *J* = 6.5, 1.9 Hz, 2H), 7.11 (dd, *J* = 6.9, 2.0 Hz, 1H), 5.85 (s, 1H), 5.21 – 5.18 (m, 1H), 2.84 – 2.75 (m, 2H), 2.20 (t, *J* = 7.6 Hz, 2H), 2.11 – 1.99 (m, 1H), 1.87 – 1.80 (m, 3H), 1.67 (p, *J* = 7.4 Hz, 2H), 1.38 – 1.25 (m, 8H), 0.93 – 0.86 (m, 3H). ^{13}C NMR (151 MHz, $CDCl_3$) δ 172.40, 137.58, 136.88, 129.15, 128.70, 127.21, 126.23, 47.27, 47.23, 37.04, 31.73, 30.24, 29.28, 29.26, 29.03, 25.93, 22.62, 20.01, 14.10. HRMS (ESI-TOF) *calcd for* $C_{18}H_{28}NO$, 274.2166 ($M+H^+$), found 274.2175.

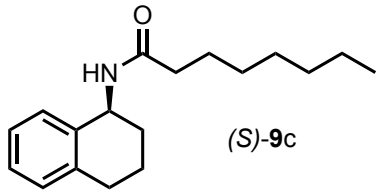

(S)-**9**c

(S)-N-(1,2,3,4-tetrahydronaphthalen-1-yl)octanamide (**S9c**): Synthesized according to general procedure 1. The residue obtained was purified by Biotage® (Hexanes/EtOAc, 7:3) to afford **S9c** as a colorless liquid (16.6 mg, 75%). ^1H NMR (600 MHz, $CDCl_3$) δ 7.26 (dd, J = 6.7, 2.3 Hz, 1H), 7.18 (dd, J = 7.3, 1.9 Hz, 2H), 7.11 (dd, J = 7.0, 2.0 Hz, 1H), 5.87 (s, 1H), 5.19 (t, J = 8.6, Hz, 1H), 2.85 – 2.72 (m, 2H), 2.22 – 2.15 (m, 2H), 2.11 – 1.97 (m, 1H), 1.91 – 1.76 (m, 3H), 1.69 – 1.63 (m, 2H), 1.41 – 1.20 (m, 8H), 0.91 (t, J = 6.7 Hz, 3H). ^{13}C NMR (151 MHz, $CDCl_3$) δ 172.43, 137.58, 136.89, 129.15, 128.70, 127.20, 126.22, 47.27, 47.23, 37.03, 37.02, 31.74, 30.24, 29.31, 29.29, 29.27, 29.04, 25.93, 25.92, 22.62, 20.02, 14.10. HRMS (ESI-TOF) calcd for $C_{18}H_{28}NO$, 274.2166 ($M+H^+$), found 274.2175.

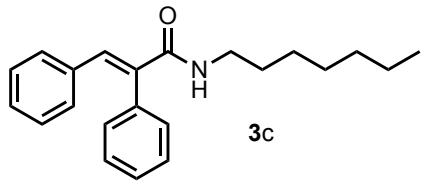

3c

(*E*)-N-heptyl-2,3-diphenylacrylamide (3c): Synthesized according to general procedure 2. The residue obtained was purified by Biotage® (Hexanes/EtOAc, 8:2) to afford **3**c as a white solid powder (17 mg, 76%). ^{1}H NMR (600 MHz, $CDCl_3$) δ 7.88 (s, 1H), 7.48 – 7.44 (m, 3H), 7.27 (d, *J* = 7.0 Hz, 2H), 7.20 – 7.12 (m, 3H), 7.00 (d, *J* = 7.5 Hz, 2H), 5.50 (s, 1H), 3.31 (q, *J* = 6.7 Hz, 2H), 1.48 – 1.43 (m, 2H), 1.32 – 1.22 (m, 8H), 0.89 (t, *J* = 6.9 Hz, 3H). ^{13}C NMR (151 MHz, $CDCl_3$) δ 166.95, 136.90, 136.88, 136.38, 135.06, 134.52, 130.34, 129.86, 129.60, 129.58, 128.50, 128.44, 128.13, 40.16, 31.69, 29.43, 28.87, 26.78, 22.55, 14.07. HRMS (ESI-TOF) calcd for $C_{22}H_{28}NO$, 322.2166 ($M+H^+$), found 322.2171.

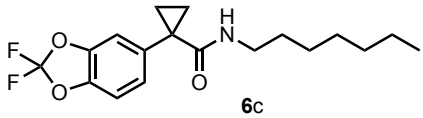

6c

1-(2,2-difluorobenzo[d][1,3]dioxol-5-yl)-N-heptylcyclopropane-1-carboxamide (6): Synthesized according to general procedure 2. The residue obtained was purified by Biotage® (Hexanes/EtOAc, 8:2) to afford **6**c as a white solid powder (16 mg, 75%). ^{1}H NMR (600 MHz, $CDCl_3$) δ 7.16 – 7.07 (m, 2H), 7.04 (d, J = 8.2 Hz, 1H), 5.23 (t, J = 5.9 Hz, 1H), 3.14 (q, J = 6.8 Hz, 2H), 1.60 – 1.56 (m, 2H), 1.40 – 1.32 (m, 2H), 1.26 – 1.18 (m, 8H), 1.01 – 0.98 (m, 2H), 0.84 (t, J = 6.9 Hz, 3H).^{13}C NMR (151 MHz, $CDCl_3$) δ 172.90, 143.91, 143.24, 136.26, 131.67, (t, J = 132 Hz) 126.37, 112.22, 109.75, 40.22, 31.66, 30.30, 29.49, 28.82, 26.71, 22.50, 15.82, 14.00. HRMS (ESI-TOF) calcd for $C_{18}H_{24}F_2NO_3$, 340.1719 ($M+H^+$), found 340.1735.

Synthesis of **3-(3-(but-3-yn-1-yl)-3H-diazirin-3-yl)-N-methylpropanamide (1), 1-(2-benzylpiperidin-1-yl)-3-(3-(but-3-yn-1-yl)-3H-diazirin-3-yl)propan-1-one (8), (R)-3-(3-(but-3-yn-1-yl)-3H-diazirin-3-yl)-1-(2-phenylpyrrolidin-1-yl)propan-1-one (*(R)*-10) , (S)-3-(3-(but-3-yn-1-yl)-3H-diazirin-3-yl)-1-(2-phenylpyrrolidin-1-yl)propan-1-one (*(S)*-10) , (R)-3-(3-(but-3-yn-1-yl)-3H-diazirin-3-yl)-N-(1,2,3,4-tetrahydronaphthalen-1-yl)propenamide (*(R)*-9) , and (S)-3-(3-(but-3-yn-1-yl)-3H-diazirin-3-yl)-N-(1,2,3,4-tetrahydronaphthalen-1-yl)propenamide (*(S)*-9)** were performed according to previously published literature procedures[5,6].

Cleavable biotin azide **Light L-Valine tag (11)** and Cleavable biotin azide **Heavy L-Valine tag (12)** are synthesized according to previously published literature procedures[7].

(1) Cleavable biotin azide light- L-Valine tag **(11)**:

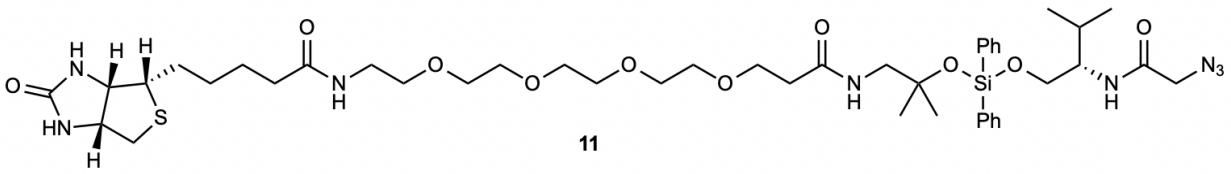

11

(2) Cleavable biotin azide heavy-L-Valine tag **(12)**:

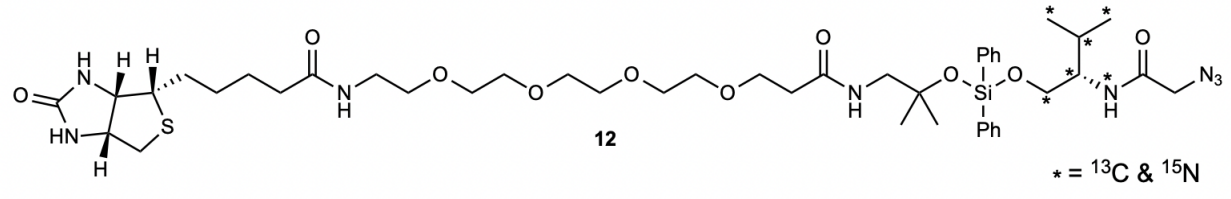

12

* = ^{13}C & ^{15}N

SI References

1 Taus, T. *et al.* Universal and confident phosphorylation site localization using phosphoRS. *J Proteome Res* **10**, 5354-5362, doi:10.1021/pr200611n (2011).

2 Potel, C. M., Lemeer, S. & Heck, A. J. R. Phosphopeptide Fragmentation and Site Localization by Mass Spectrometry: An Update. *Anal Chem* **91**, 126-141, doi:10.1021/acs.analchem.8b04746 (2019).

3 Beausoleil, S. A., Villen, J., Gerber, S. A., Rush, J. & Gygi, S. P. A probability-based approach for high-throughput protein phosphorylation analysis and site localization. *Nat Biotechnol* **24**, 1285-1292, doi:10.1038/nbt1240 (2006).

4 Savitski, M. M. *et al.* Confident phosphorylation site localization using the Mascot Delta Score. *Mol Cell Proteomics* **10**, M110 003830, doi:10.1074/mcp.M110.003830 (2011).

5 Parker, C. G. *et al.* Ligand and Target Discovery by Fragment-Based Screening in Human Cells. *Cell* **168**, 527-541 e529, doi:10.1016/j.cell.2016.12.029 (2017).

6 Wang, Y. *et al.* Expedited mapping of the ligandable proteome using fully functionalized enantiomeric probe pairs. *Nat Chem* **11**, 1113-1123, doi:10.1038/s41557-019-0351-5 (2019).

7 Conway, L. P. *et al.* Evaluation of fully-functionalized diazirine tags for chemical proteomic applications. *Chem Sci* **12**, 7839-7847, doi:10.1039/d1sc01360b (2021).

NMR spectra

^{1}H NMR ($CDCl_3$) **2**

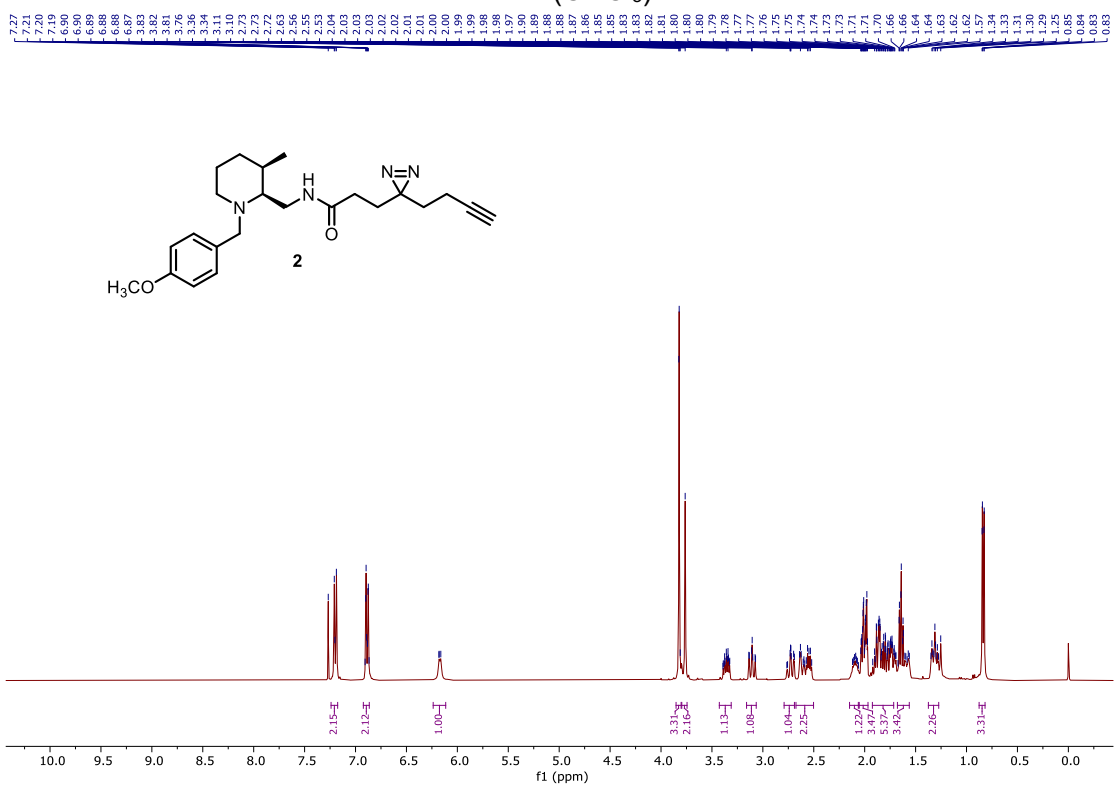

^{13}C NMR ($CDCl_3$) **2**

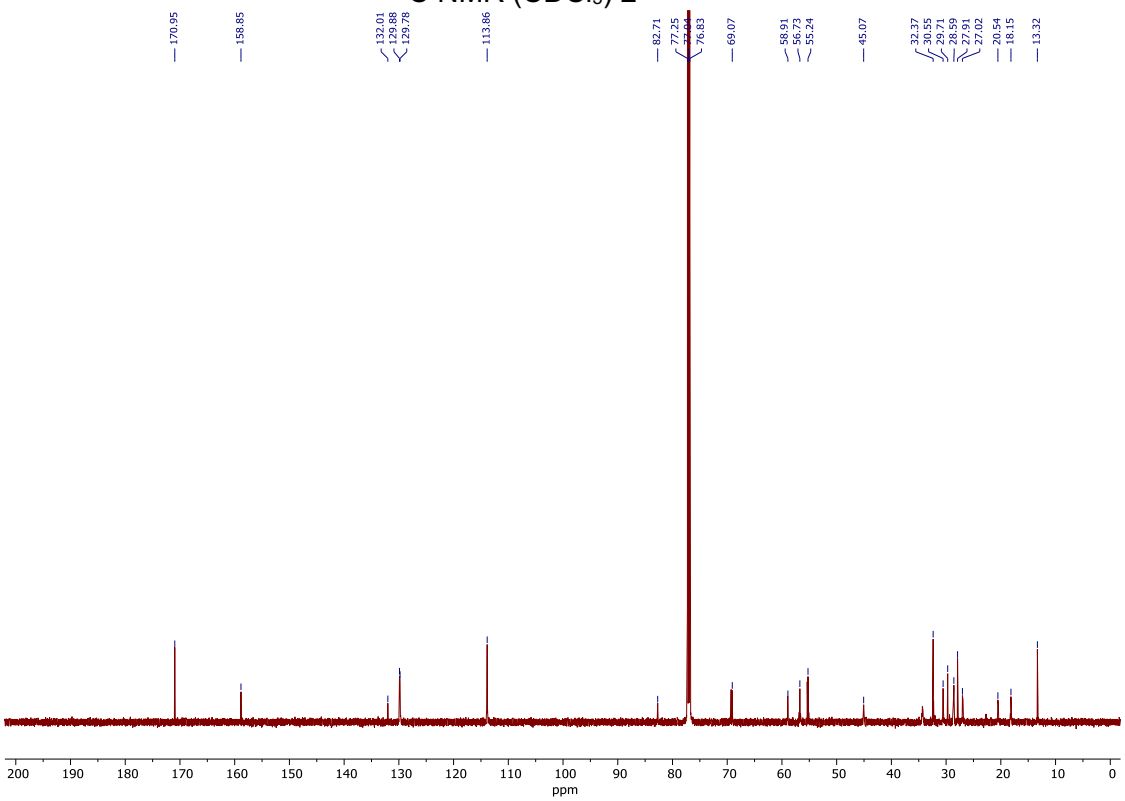

^{1}H NMR ($CDCl_3$) **3**

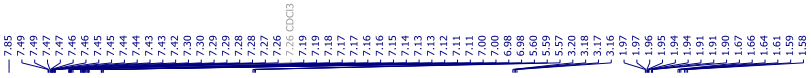

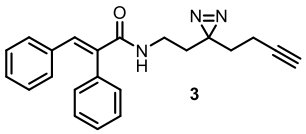

3

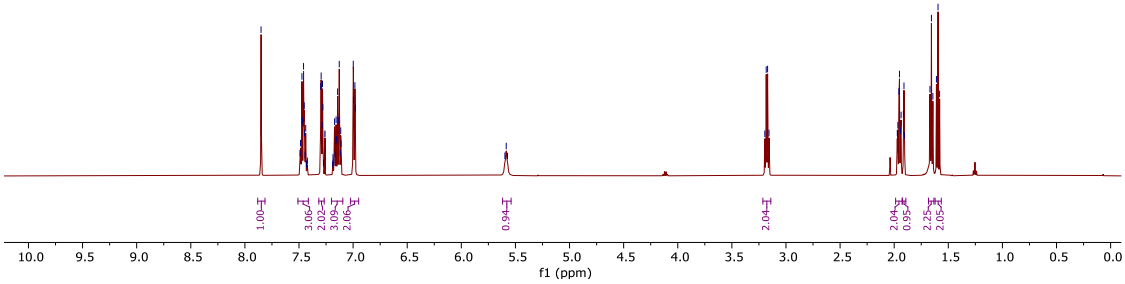

^{13}C NMR ($CDCl_3$) **3**

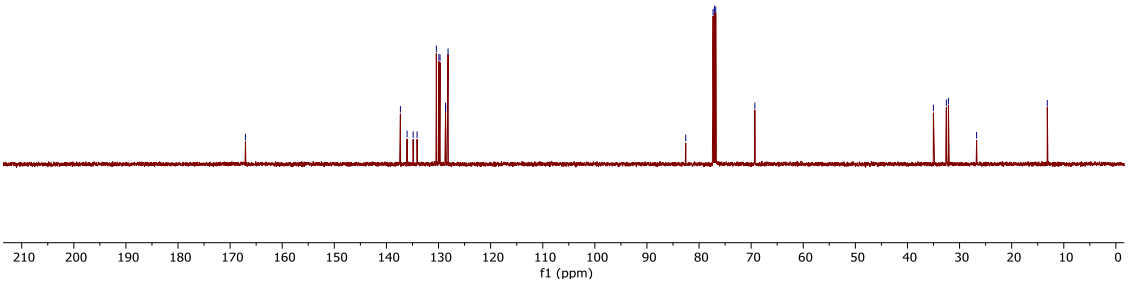

^{1}H NMR ($CDCl_3$) **4**

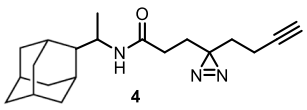

4

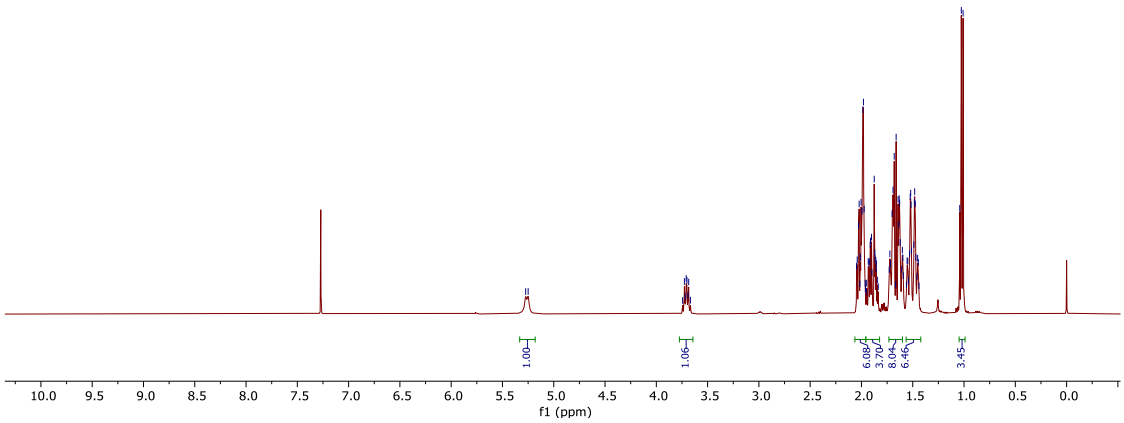

^{13}C NMR ($CDCl_3$) **4**

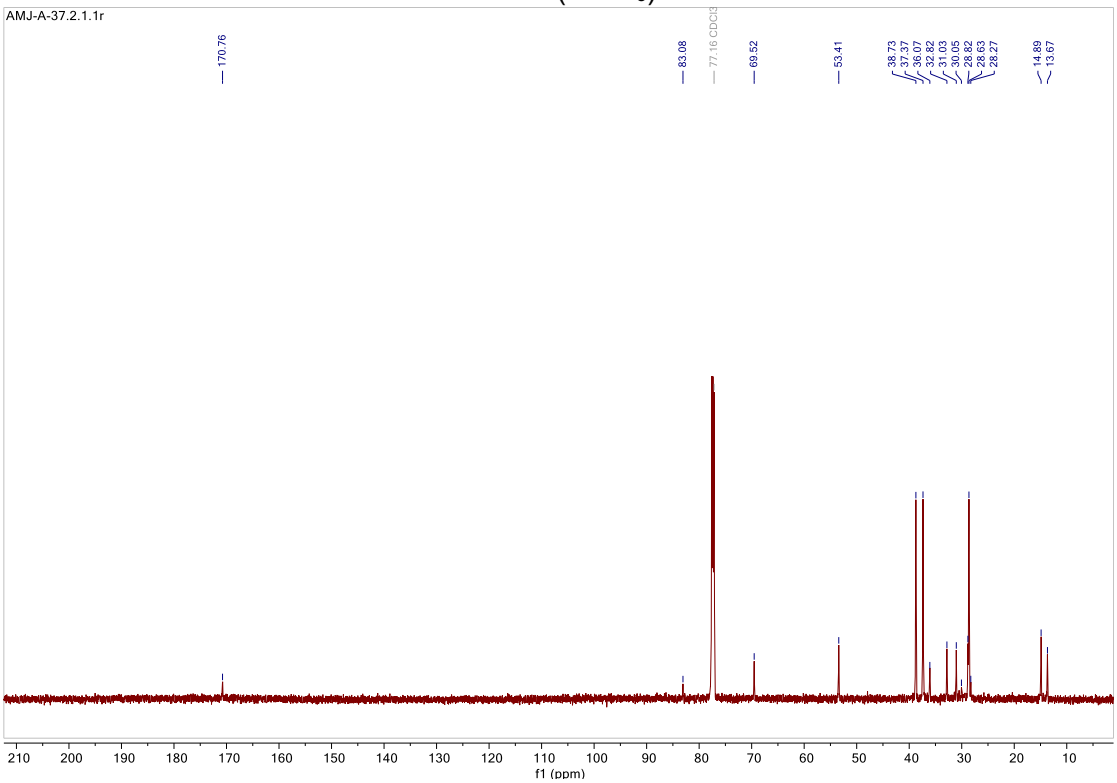

^{1}H NMR ($CDCl_3$) **5**

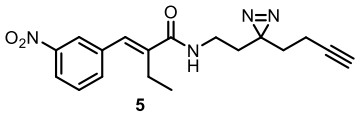

5

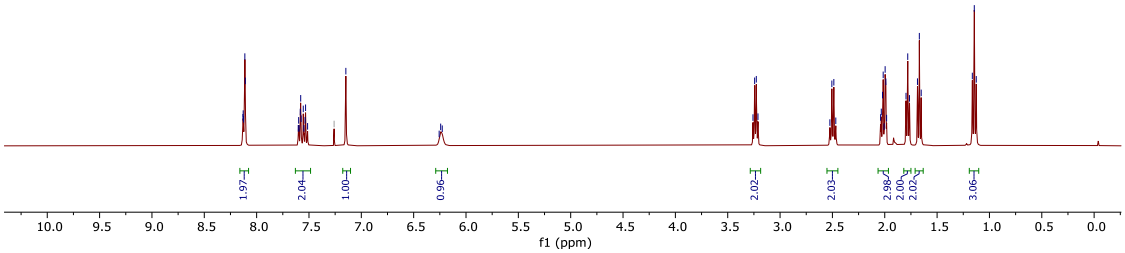

^{13}C NMR ($CDCl_3$) **5**

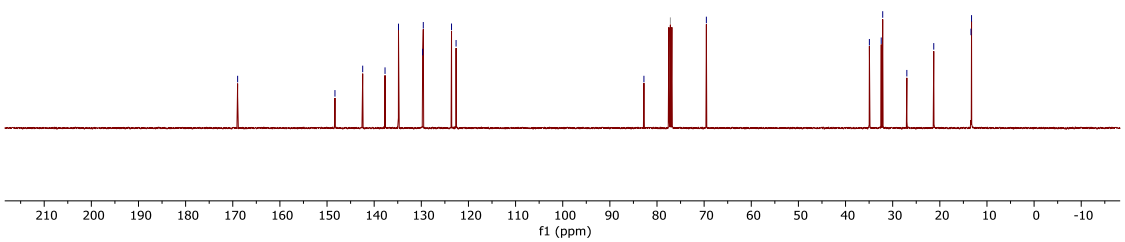

^{1}H NMR ($CDCl_3$) **6**

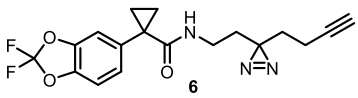

6

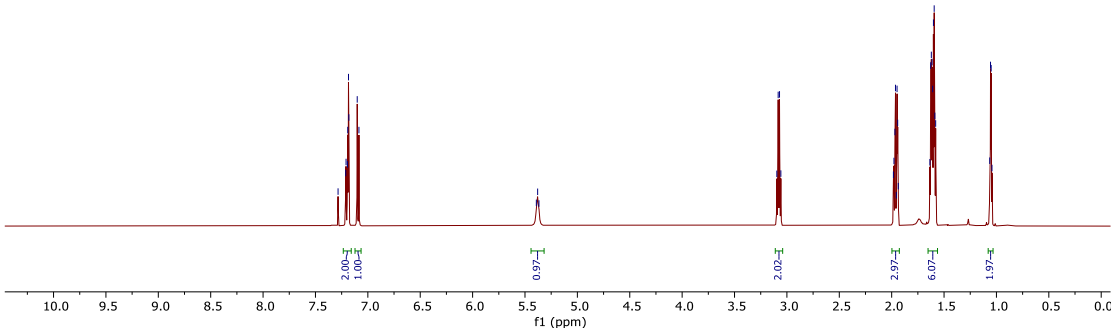

^{13}C NMR ($CDCl_3$) **6**

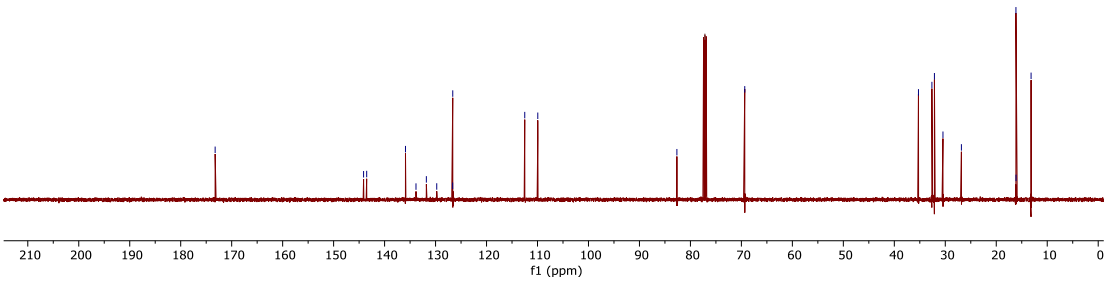

^{1}H NMR ($CDCl_3$) **7**

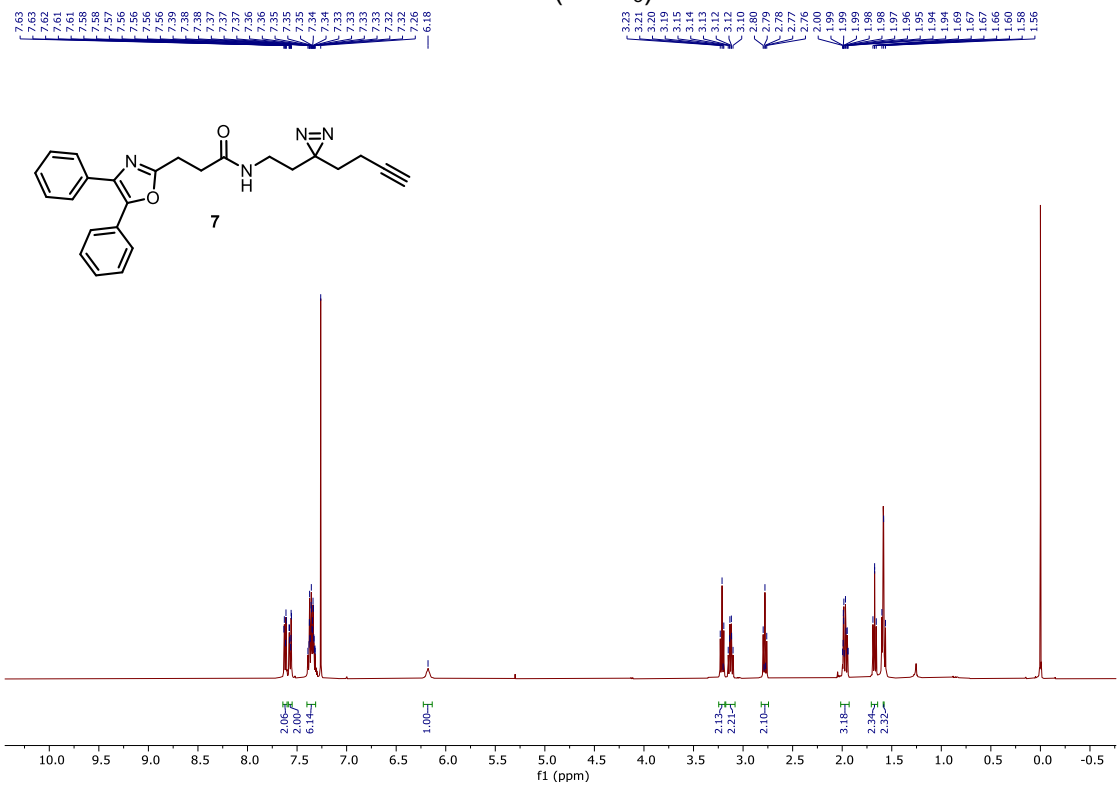

^{13}C NMR ($CDCl_3$) **7**

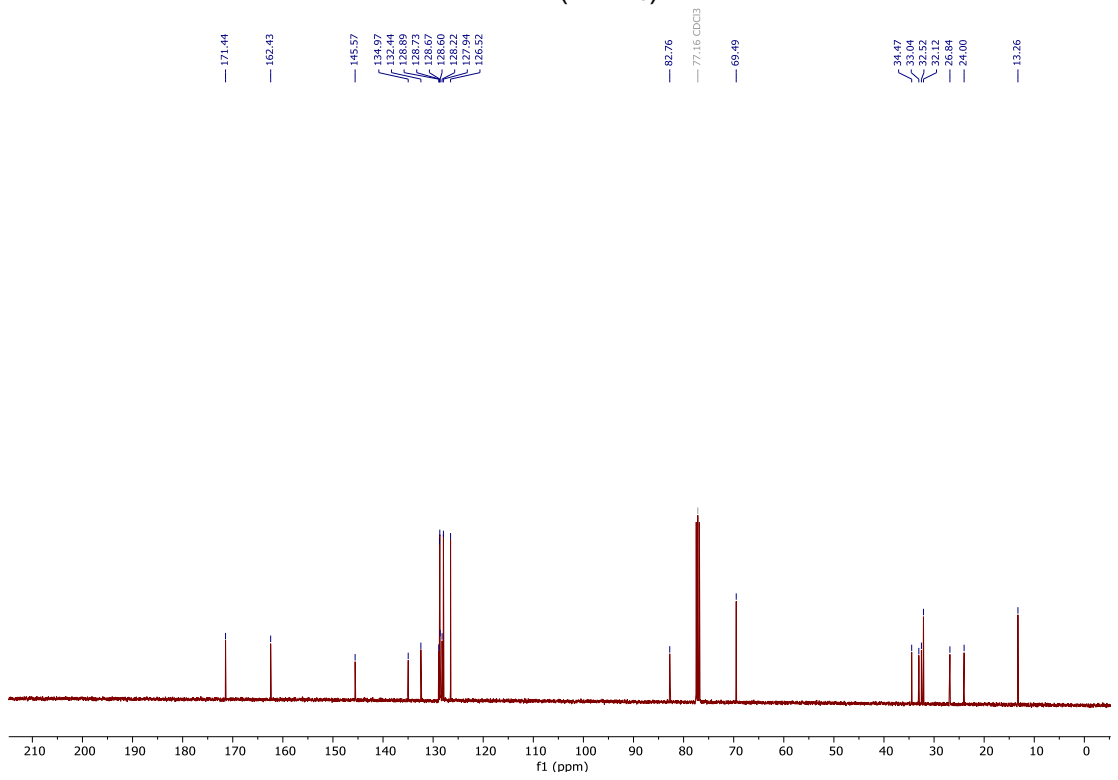

^{1}H NMR ($CDCl_3$) **3c**

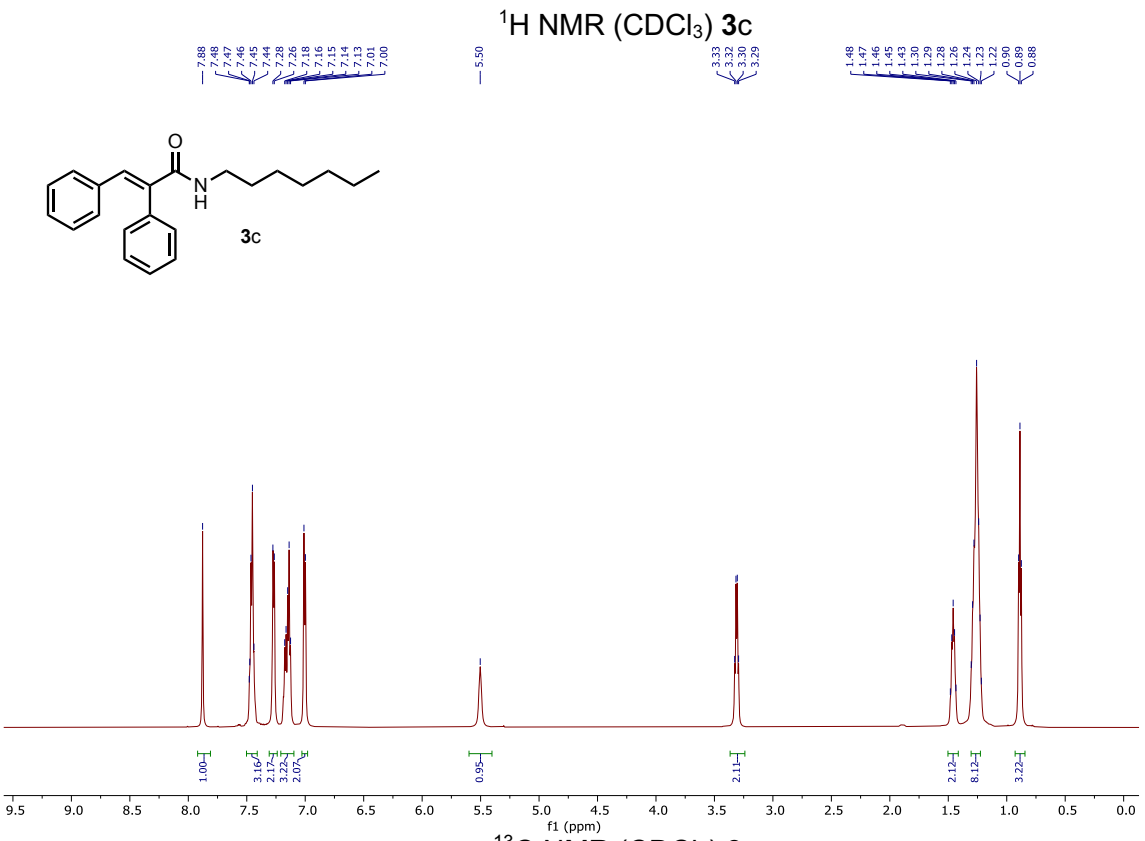

^{13}C NMR ($CDCl_3$) **3c**

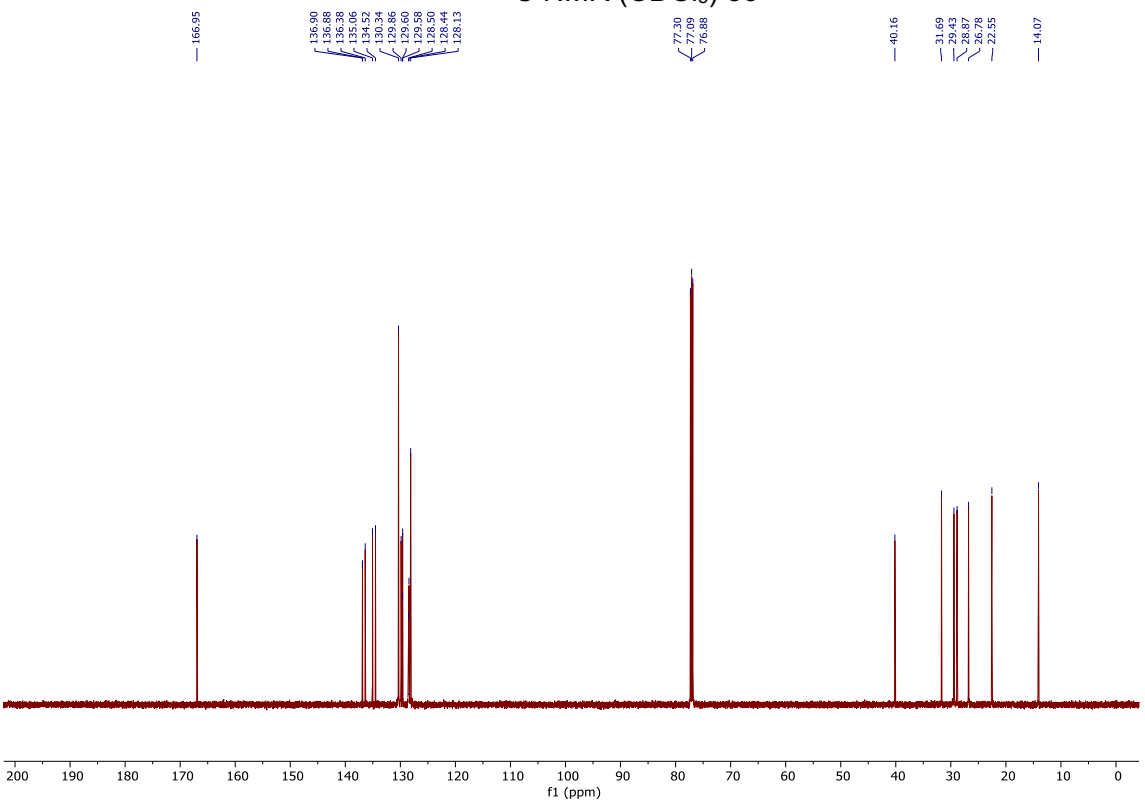

^{1}H NMR ($CDCl_3$) **6c**

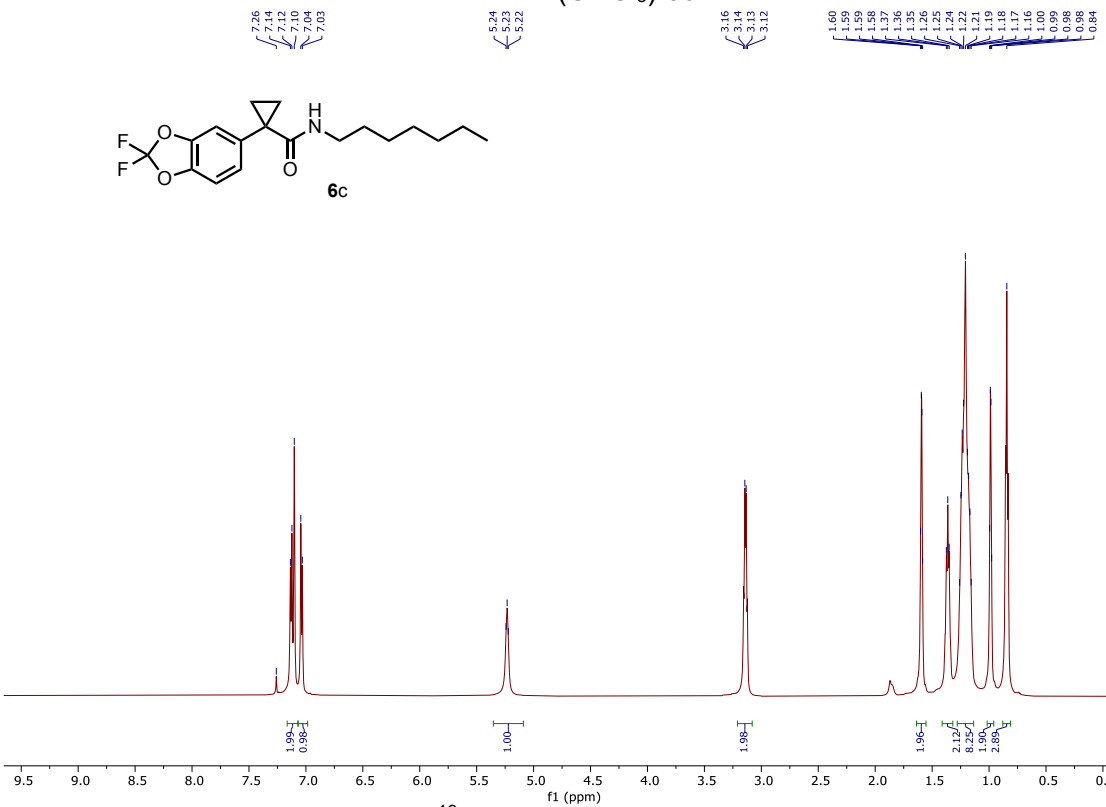

^{13}C NMR ($CDCl_3$) **6c**

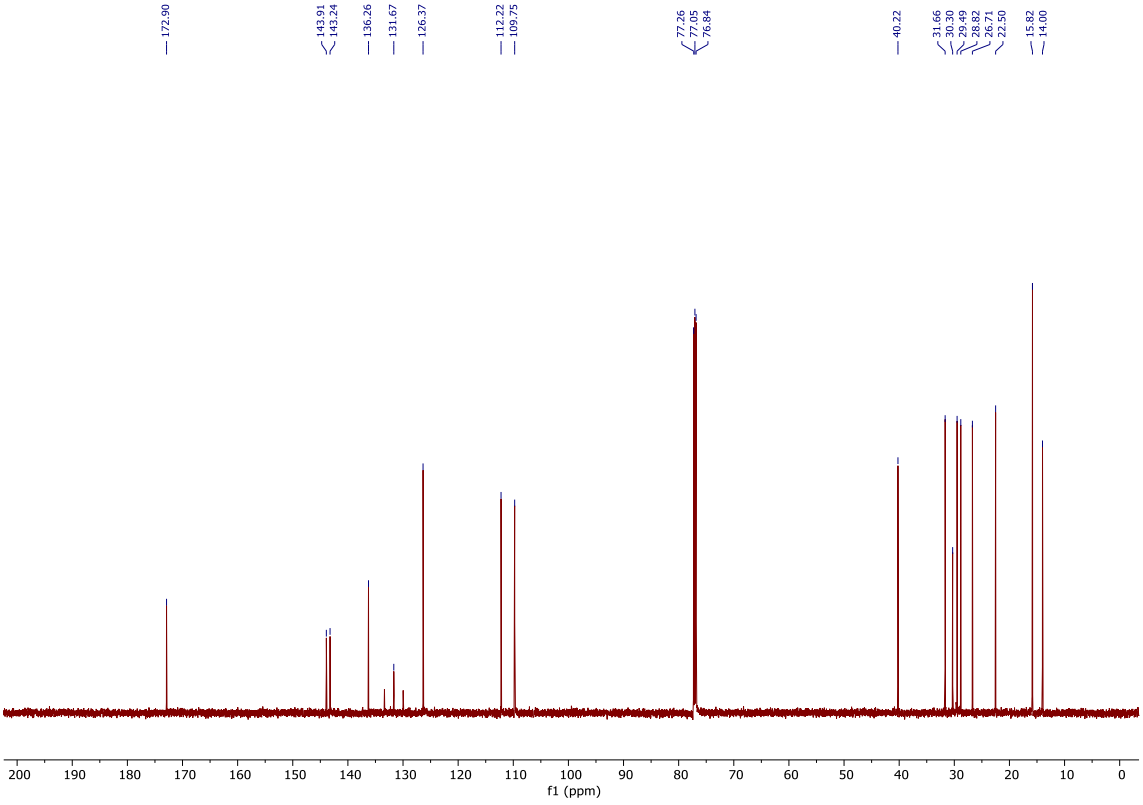

^{1}H NMR ($CDCl_3$) (*R*)-**9c**

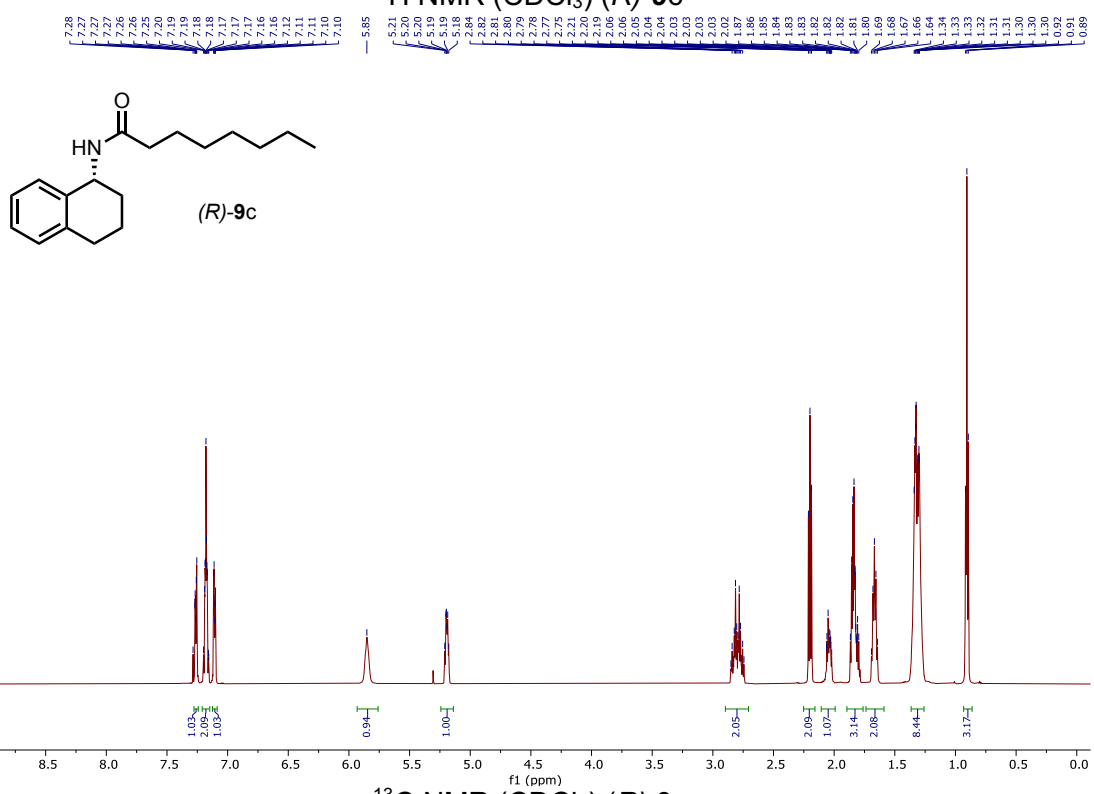

^{13}C NMR ($CDCl_3$) (*R*)-**9c**

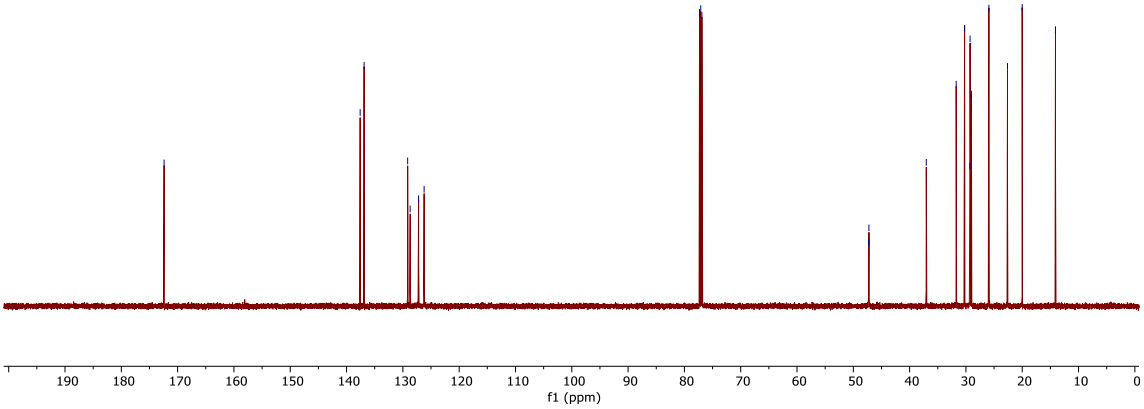

^{1}H NMR ($CDCl_3$) (*S*)-**9c**

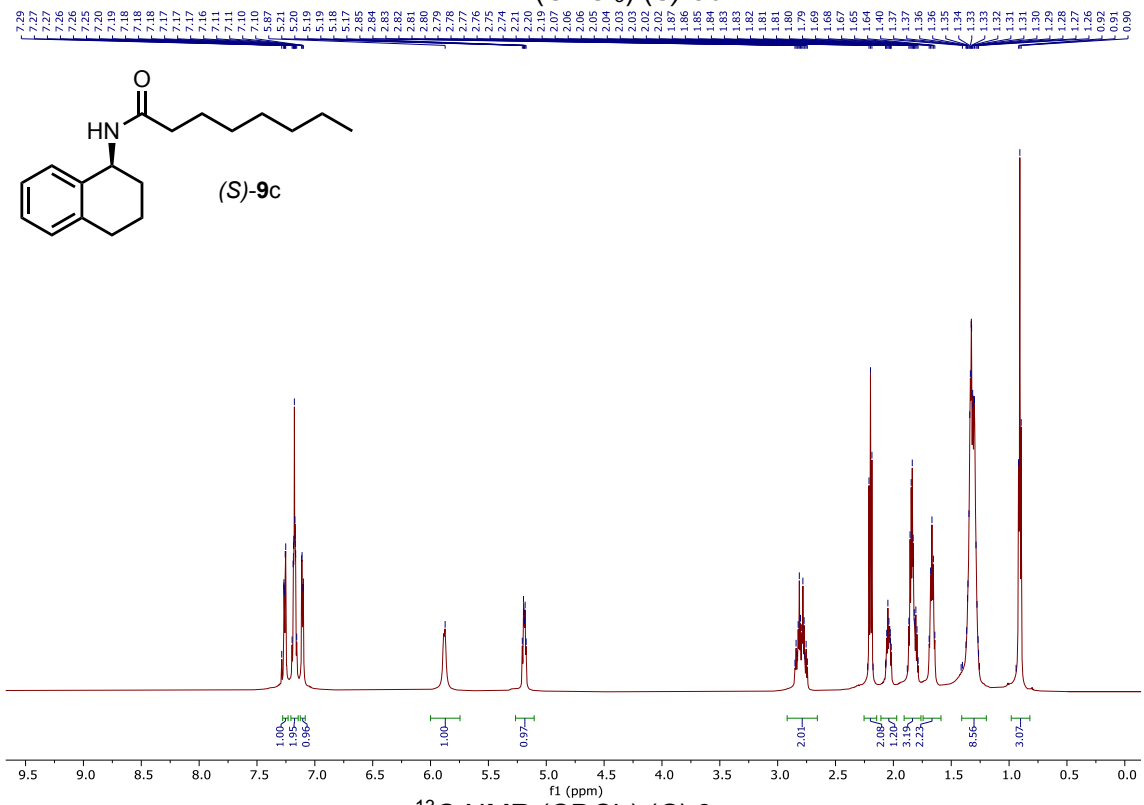

^{13}C NMR ($CDCl_3$) (*S*)-**9c**